

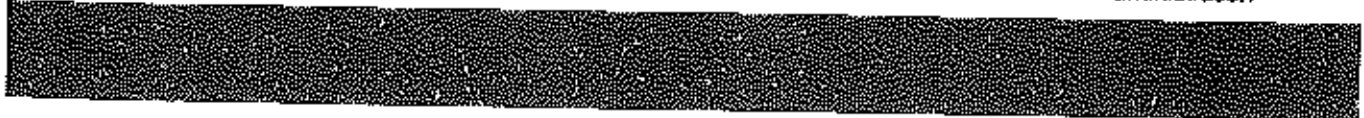
# PROCEDURES FOR CALCULATING FIELD INTENSITIES OF ANTENNAS



***technical memorandum series***

---

U.S. DEPARTMENT OF COMMERCE • National Telecommunications and Information Administration



# PROCEDURES FOR CALCULATING FIELD INTENSITIES OF ANTENNAS

ANDREW FARRAR  
EUGENE CHANG



**U.S. DEPARTMENT OF COMMERCE**  
**Bruce Smart, Acting Secretary**

Alfred C. Sikes, Assistant Secretary  
for Communications and Information

**SEPTEMBER 1987**

## ABSTRACT

This report discusses simplified procedures for calculating near and far field intensities of several types of aperture and wire antennas. The antenna technical characteristics listed in the Government Master File (GMF) were reviewed. For this analysis, two categories (i.e., linear and aperture) were found to be sufficiently representative of the majority of antenna types listed in the GMF. Existing analytical antenna models developed for a near field analysis of the antennas were identified. Some of these models were used to develop a simplified model for estimating near field radiation from Government radiocommunications systems. These models are conservative and are expected to yield higher field intensity or power density values than would be expected in actual practice. Measurements may be required to determine more exact values for these parameters.

## KEY WORDS

Antennas

Computer Models

Linear and Aperture Antennas

Models for Near Field Analysis

Near Field Analysis of Antennas

Radio Frequency Radiation Hazard Assessment

TABLE OF CONTENTS

<u>Subsection</u>	<u>Page</u>
SECTION 1	
INTRODUCTION	
BACKGROUND .....	1-1
OBJECTIVES .....	1-2
APPROACH .....	1-2

SECTION 2  
CONCLUSIONS AND RECOMMENDATIONS

GENERAL .....	2-1
SPECIFIC CONCLUSIONS .....	2-2
RECOMMENDATIONS .....	2-2

SECTION 3  
DATA BASE

GENERAL .....	3-1
ANTENNA TYPES .....	3-2

TABLE OF CONTENTS (continued)

<u>Subsection</u>	<u>Page</u>
SECTION 4	
ANALYSIS	
ANALYSIS PROCEDURES .....	4-1
COMPUTER MODELS .....	4-2
Numerical Electromagnetic Code -- Reflector Antenna .....	4-4
Numerical Electromagnetic Code (NEC) .....	4-5
SIMPLIFIED MODELS FOR NEAR FIELD CALCULATIONS .....	4-9
Aperture Antennas .....	4-9
Correction Factors for Circular Apertures .....	4-10
Relationships Between n and Far Field Characteristics .....	4-15
Off-Axis Power Density For Circular Apertures.....	4-18
Correction Factors for Rectangular Apertures .....	4-20
Relationships Between n and Far Field Characteristics .....	4-22
Applications of Analysis Procedure .....	4-38
Linear Antenna .....	4-41
Some Thoughts on Near Field Calculations of Wire Antennas .....	4-42
Dipole Antenna .....	4-43
Monopole .....	4-50
Whip .....	4-50
Log Periodic .....	4-52
Yagi Antenna .....	4-55
Collinear Antennas .....	4-59
Summary of Results .....	4-61

TABLE OF CONTENTS (continued)

LIST OF TABLES

<u>Table</u>		<u>Page</u>
3-1	CATEGORIZATION OF ANTENNAS USED BY THE MAJORITY OF THE GOVERNMENT TELECOMMUNICATION SYSTEMS .....	3-3
4-1	FAR FIELD PATTERN CHARACTERISTICS PRODUCED BY A DISTRIBUTION $(1-p^2)^n$ OVER A CIRCULAR APERTURE .....	4-17
4-2	RELATIONSHIPS FOR ON-AXIS POWER DENSITY CALCULATIONS FOR RECTANGULAR APERTURES .....	4-21
4-3	FAR FIELD CHARACTERISTICS OF RECTANGULAR APERTURES WITH $\cos^n \frac{\pi x}{2a}$ DISTRIBUTION FUNCTIONS .....	4-36
4-4	FAR FIELD CHARACTERISTICS OF RECTANGULAR APERTURES WITH $\cos^n \frac{\pi x'}{2a} \cos^n \frac{\pi y'}{2b}$ DISTRIBUTION FUNCTIONS .....	4-37
4-5	DESCRIPTION OF PARAMETERS USED IN EQUATIONS 4-16, 4-17 ...	4-63

LIST OF FIGURES

<u>Figure</u>		<u>Page</u>
4-1	Correction factor vs. on axis distance normalized to $2D^2/\lambda$ for a circular aperture with uniform distribution, (a) $D/\lambda = 20$ , (b) $D/\lambda = 40$ .....	4-12

TABLE OF CONTENTS (continued)

LIST OF FIGURES (continued)

<u>Figure</u>		<u>Page</u>
4-2	Correction factor vs. on-axis distance normalized to $2D^2/\lambda$ for circular apertures with tapered distribution, ( $D/\lambda = 20$ ), (a) $n = 0.5$ , (b) $n = 1.0$ , (c) $n = 1.5$ , (d) $n = 2.0$ , (e) $n = 2.5$ , and (f) $n = 3.0$ .....	4-13
4-3	Correction factor vs. on-axis distance normalized to $2D^2/\lambda$ for circular apertures with tapered distribution, ( $D/\lambda = 40$ ), (a) $n = 0.5$ , (b) $n = 1.0$ , (c) $n = 1.5$ , (d) $n = 2.0$ , (e) $n = 2.5$ , and (f) $n = 3.0$ .....	4-14
4-4	Maximum correction factor vs. on-axis distance normalized to $2D^2/\lambda$ for circular apertures, (a) $D/\lambda = 20$ , (b) $D/\lambda = 40$ ..	4-16
4-5	Data for off-axis calculation of power density, (a) regions close to the antenna, (b) regions further away from antenna .....	4-19
4-6	Correction factor vs. on-axis distance normalized to $8a^2/\lambda$ for rectangular aperture with dimensions $a/\lambda = 20$ , $b/\lambda = 10$ , and different distribution functions .....	4-23
4-7	Correction factor vs. on-axis distance normalized to $8a^2/\lambda$ for rectangular aperture with dimensions $a/\lambda = 30$ , $b/\lambda = 10$ , and different distribution functions .....	4-24

TABLE OF CONTENTS (continued)

LIST OF FIGURES (continued)

<u>Figure</u>	<u>Page</u>
4-8      Correction factor vs. on-axis distance normalized to $8a^2/\lambda$ for rectangular aperture with dimensions $a/\lambda = 40$ , $b/\lambda = 20$ , and different distribution functions .....	4-25
4-9      Correction factor vs. on-axis distance normalized to $8a^2/\lambda$ for rectangular aperture with dimensions $a/\lambda = 40$ , $b/\lambda = 30$ , and different distribution functions .....	4-26
4-10     Correction factor vs. on-axis distance normalized to $8a^2/\lambda$ for rectangular aperture with dimensions $a/\lambda = 20$ , $b/\lambda = 20$ , and different distribution functions .....	4-27
4-11     Correction factor vs. on-axis distance normalized to $8a^2/\lambda$ for rectangular aperture with dimensions $a/\lambda = 5$ , $b/\lambda = 5$ , and different distribution functions .....	4-28
4-12     Correction factor vs. on-axis distance normalized to $8a^2/\lambda$ for rectangular aperture with dimensions $a/\lambda = 10$ , $b/\lambda = 5$ , and different distribution functions .....	4-29
4-13     Correction factor vs. on-axis distance normalized to $8a^2/\lambda$ for rectangular aperture with dimensions $a/\lambda = 10$ , $b/\lambda = 10$ , and different distribution functions .....	4-30



TABLE OF CONTENTS (continued)

LIST OF FIGURES (continued)

<u>Figure</u>		<u>Page</u>
4-14	Correction factor vs. on-axis distance normalized to $8a^2/\lambda$ for rectangular aperture with dimensions $a/\lambda = 15$ , $b/\lambda = 5$ , and different distribution functions .....	4-31
4-15	Correction factor vs. on-axis distance normalized to $8a^2/\lambda$ for rectangular aperture with dimensions $a/\lambda = 15$ , $b/\lambda = 10$ , and different distribution functions .....	4-32
4-16	Correction factor vs. on-axis distance normalized to $8a^2/\lambda$ for rectangular aperture with dimensions $a/\lambda = 15$ , $b/\lambda = 15$ , and different distribution functions .....	4-33
4-17	Correction factor vs. on-axis distance normalized to $8a^2/\lambda$ for rectangular aperture with dimensions $a/\lambda = 20$ , $b/\lambda = 5$ , and different distribution functions .....	4-34
4-18	Correction factor vs. on-axis distance normalized to $8a^2/\lambda$ for rectangular aperture with dimensions $a/\lambda = 20$ , $b/\lambda = 15$ , and different distribution functions .....	4-35
4-19	Geometry of a short electric dipole antenna .....	4-44
4-20	Geometry for a dipole antenna .....	4-46

TABLE OF CONTENTS (continued)

LIST OF FIGURES

(Continued)

<u>Figure</u>		<u>Page</u>
4-21	A plot of the normalized electric field along the y-axis .	4-46
4-22	Correction factor vs. distance normalized to 1.5 $\lambda$ away from a half-wave dipole in free space, (a) electric field, (b) magnetic field .....	4-48
4-23	Correction factor vs. distance normalized to 1.5 $\lambda$ away from a full-wave dipole in free space, (a) electric field, (b) magnetic field .....	4-49
4-24	The monopole antenna geometry .....	4-50
4-25	Three different types of whip antennas designed for use on vehicles .....	4-51
4-26	Structures of an H.F. log periodic antenna .....	4-52
4-27	Log-periodic wire trapezoid antenna .....	4-53
4-28	Comparison of normalized field intensity of electric dipole with that produced by an eight or 12 element log periodic antenna .....	4-54
4-29	A six-element Yagi antenna .....	4-56
4-30	Comparison of correction factor for a single dipole with that of a Yagi antenna .....	4-58

TABLE OF CONTENTS (continued)

LIST OF FIGURES (continued)

<u>Figure</u>		<u>Page</u>
4-31	Design of a collinear antenna .....	4-59
4-32	Comparison of correction factor for E and H fields of a collinear antenna with full-wave dipole .....	4-60
A-1	Rectangular aperture geometry .....	A-2

LIST OF APPENDIXES

Appendix

A	DEFINITION OF THE PARAMETERS IN TABLE 4-2.....	A-1
B	COMPUTER PROGRAMS FOR CALCULATION OF NORMALIZED POWER DENSITY (CORRECTION FACTOR).....	B-1

	BIBLIOGRAPHY	C-1
--	--------------	-----

	LIST OF REFERENCES	E-1
--	--------------------	-----

## SECTION 1

### INTRODUCTION

#### BACKGROUND

The National Telecommunications and Informations Administration (NTIA) is responsible for managing the Federal Government's use of the radio spectrum. Part of NTIA's responsibility is to establish policies concerning spectrum assignment, allocation and use, and provide the various Departments and agencies with guidance to ensure that their conduct of telecommunications activities is consistent with these policies [NTIA, 1986].

Federal agencies operating radiocommunications systems and NTIA, which authorizes the Federal Government's use of the RF spectrum, need simple and easy-to-use analytical procedures for assessing whether these operations conform to RF radiation protection criteria. Similarly, procedures for measuring power density levels in the vicinity of government transmitters may be required for confirmation to assess the compliance of systems that have been installed. In addition, measurement procedures are necessary for assessing potential exposures from antennas; however, the calculation procedures discussed here cannot be applied.

A very careful calculation/prediction of power densities in the near field of any transmitting antenna must use a complex model, usually implemented on a computer, developed specifically for that antenna. Such a custom designed model can only be used with detailed antenna parameters that are seldom available at the time when frequency assignment and spectrum support decisions must be made. Furthermore, the detailed calculations, even when using a computer, are quite complex and require technical judgment.

The Spectrum Engineering and Analysis Division (SEAD) of NTIA has been requested to develop conservative, easy to use estimators of power density in both the near and far fields of transmitting antennas often used in government systems. Existing mathematical models are used to develop suitable estimators. The estimators will be coordinated with other regulatory agencies having responsibilities in this area (e.g., Environmental Protection Agency

(EPA) and Federal Communications Commission (FCC)) and with government users of the spectrum to foster a common understanding of this approach to determining conformance with any exposure criteria.

#### OBJECTIVES

The objectives of this effort were to:

1. identify the appropriate available computer and other analytical models for the near field calculations of antennas
2. determine the advantages and limitations of the models in item 1 above
3. evaluate the applicability of the models in providing simplified procedures useful to the near field analysis
4. develop simple procedures for estimating the near and far field intensities of antennas often used in government telecommunications systems
5. compile an annotated bibliography.

#### APPROACH

To accomplish the objectives discussed above, the following approach was used.

A literature search was made to identify useful and appropriate computer and other analytical models. The models were examined and used in the selection and development of simple procedures for computation of the near field intensities related to the radiation hazard analysis.

The need for simple procedures and the availability of the necessary data, as well as the type of data presently recorded in the Government Master File (GMF) and similar data bases, were key factors in the selection of the models discussed in this report.

A bibliography was developed to provide additional information, such as methods to assist in calculating fields of specific antennas.

## SECTION 2

### CONCLUSIONS AND RECOMMENDATIONS

#### GENERAL

NTIA and other government agencies involved in the management or use of the radio frequency spectrum need to assess potential RF radiation exposures associated with government radiocommunications systems. Technical characteristics of the antennas used by these systems, especially field intensities in the near field produced by them, are among the key factors in carrying out this assessment. To this end, simplified procedures for estimating the near field of antennas were developed. Two general categories of antennas were identified, aperture and linear, and procedures for each category were prepared. These procedures are presented as a baseline approach. They are simple to follow and require no data beyond those submitted by agencies for the system review process. These procedures provide results useful in checking the compliance of a system with radiation hazard criteria; however, other methods and procedures, based on sound engineering practice for evaluating compliance can be used.

The procedures developed here are applicable to isolated systems. The cases of multiple emitters and antenna arrays (except collinear arrays) were not addressed during this effort. However, the procedures are applicable to a large number of radiocommunications systems used by the government. Additional efforts are required to extend these procedures or develop new capabilities to treat the antenna types not included in this analysis.

These procedures, with the exception of those for some of the linear antennas, are based on existing models generally used by some government agencies. Limitations and advantages are described. These procedures are subject to further refinement.

## SPECIFIC CONCLUSIONS

1. The analysis results indicate that for the purpose of estimating the field intensity of antennas, it is feasible to group the majority of the antennas included in the GMF into either a linear or an aperture category as indicated in TABLE 3-1.
2. The simple procedure developed here for both aperture and linear antennas may be used to assess the near and/or far field intensities of antennas used in government radiocommunications systems.
3. Additional efforts are needed to extend the procedure to the antenna types listed in TABLE 3-1, which are not discussed in this analysis.
4. The data on antenna characteristics requested on NTIA Form 35 and provided by the federal agencies for system reviews were found to be sufficient for the application of the procedures developed here.
5. These simplified procedures may be used for evaluating the compliance of government radiocommunications systems with radiation hazard criteria.
6. The data in the GMF often does not include parameters needed for the analysis procedures discussed here, such as beamwidth and sidelobe levels.

## RECOMMENDATIONS

The following are NTIA staff recommendations based on the technical findings contained in this report. Any action to implement these recommendations will be accomplished under separate correspondence. It is recommended that the following be done by NTIA:

1. coordinate the procedures described in this report with the IRAC agencies to develop baseline methods for the calculations of the near field
2. use the procedures given here when assessing compliance of Government radiocommunications systems with radiation hazard criteria

3. continue improving the procedures for more accuracy and validate them through laboratory and/or field measurements
4. extend the analysis procedures to include the antennas not treated in this report.



## SECTION 3

### DATA BASE

#### GENERAL

For estimating field intensities using the procedures discussed here, the information in Form NTIA 33 and 35 is adequate. More accurate assessment of the field intensities requires much more detailed information, such as antenna dimensions, height above terrain, beam shaping, objects in the near field, that is difficult to obtain. These procedures can be used with data normally provided with system review requests and do not require the development of a data base for near field analysis. The data available to NTIA in existing data bases which could be used for near field analysis were important in determining useful and simplified procedures for near field calculations by the NTIA.

The GMF was used to categorize antennas used in Government radiocommunication systems and to identify the information which was available to calculate field intensities. The antenna characteristics in the GMF and Form NTIA 35 are described below. Categorization of antennas as linear and aperture based on a GMF selection is also described.

The Government Master File (GMF) is maintained according to the frequency assignment principles outlined in the NTIA Manual. The GMF is a data file of frequency assignments authorized to Government agencies.

Compliance with the procedures for the system review of a radiocommunications system requires the submitting agencies to file three forms (NTIA-33, NTIA-34, and NTIA-35) which contain information on equipment characteristics. Form NTIA-35, "Antenna Equipment Characteristics" contains technical and operational data on the system antenna(s). The following information required to use the procedures in this report is included in Form NTIA 33 and 35:

1. System Nomenclature
2. Frequency Range
3. Transmitter Power Output
4. Antenna Type
5. Gain: (a) Main Beam (b) Sidelobe
6. Beamwidth: (a) Horizontal (b) Vertical
7. Polarization
8. Scan Characteristics

All the data except for 5(b) and 6 can be generally found in the GMF. In practice, sometimes information for some of the items listed above for a given system may be missing in the GMF, because the data is classified or because Section 9.8.2 of the NTIA Manual makes submission of some antenna characteristic data optional for certain frequency uses.

#### ANTENNA TYPES

There was a total of approximately 216,000 assignments in the GMF, at the time of this analysis, representing a large number of telecommunication systems owned by the Federal Government. The number of assignments does not match the number of transmitters. There are often several stations for each assignment. The GMF was used to identify the variety of antennas used by the Government based on over 100,000 assignment records.

Using a computerized selection process, a list was made of transmitting antennas having unique names in the GMF together with the number of occurrences of each name. Not including the transmitting antennas (names) occurring less than ten times 46 distinct types were found to be used in 100,762 assignments in the GMF. This represents 75% of the assignments that have an antenna name recorded in the GMF. These antennas are listed in TABLE 3-1.

TABLE 3-1  
 CATEGORIZATION OF ANTENNAS USED BY THE  
 MAJORITY OF THE GOVERNMENT TELECOMMUNICATION  
 SYSTEMS (April, 1986)

<u>TYPE</u>	<u>CATEGORY</u>	<u>COUNT</u>	<u>PERCENT</u>
ARRAY	LINEAR/APERTURE	242	.24%
BICONICAL	LINEAR	119	.32%
BLADE	LINEAR	1623	1.61%
BROADBAND	LINEAR	528	.52%
CARDIOID	LINEAR	216	.21%
CASSEGRAIN*	APERTURE	56	.06%
COAXIAL	LINEAR	1984	1.97%
COLLINEAR*	LINEAR	24320	24.13%
COLLINEAR ARRAY	LINEAR	951	.94%
CONICAL	LINEAR	101	.10%
CORNER REFLECTOR	APERTURE	2764	2.75%
DIPOLE*	LINEAR	9147	9.58%
DIPOLE ARRAY	LINEAR/APERTURE	3066	3.04%
DISCONE	LINEAR	2688	2.67%
DISH*	APERTURE	35	.03%
FOLDED COAXIAL	LINEAR	193	.19%
FOLDED DIPOLE	LINEAR	1095	1.09%
GROUND-PLANE	LINEAR	5370	5.33%
HELIX	LINEAR	381	.38%
HORN*	APERTURE	882	.88%
LENS	APERTURE	19	.02%
LOG PERIODIC*	LINEAR	876	.87%
LOOP	LINEAR	41	.04%
MICROSTRIP	LINEAR	57	.06%
MONOPOLE*	LINEAR	1514	1.50%
OMNI-DIRECTIONAL	LINEAR	737	.73%
PARABOLIC CYLINDER*	APERTURE	33	.03%
PARABOLIC REFLECTOR*	APERTURE	368	.37%
PARABOLOID	APERTURE	17305	17.17%
PHASED ARRAY	APERTURE	202	.20%
PILLBOX	APERTURE	243	.24%
PLANAR ARRAY	APERTURE	103	.10%
QUARTER-WAVE	LINEAR	196	.19%
RHOMBIC	LINEAR	237	.23%
SLOT	LINEAR	204	.20%
SLOTTED ARRAY	LINEAR/APERTURE	364	.36%
SPIRAL	LINEAR	25	.02%
STACKED ARRAY	LINEAR	946	.94%
STACKED DIPOLE	LINEAR	2034	2.02%
STUB	LINEAR	624	.62%
SWASTIKA	LINEAR	119	.12%
TRAVELING-WAVE	LINEAR	194	.19%
VERTICAL DIPOLE	LINEAR	1707	1.69%
VERTICAL RADIATOR	LINEAR	155	.15%
WHIP*	LINEAR	10581	10.50%
YAGI*	LINEAR	6122	6.08%

-----  
 \* Indicates the antenna types considered in the analysis.

For this analysis, it is convenient to group the antennas into two broad categories: linear and aperture. Each antenna in the GMF is categorized as linear or aperture. The category entitled "linear/aperture" in TABLE 3-1 may be considered as linear or aperture for the purpose of analysis.

In the linear category, the emphasis in this report was on wire antennas operating at frequencies from 10 MHz to 1.2 GHz. Those with asterisks in TABLE 3-1 were occurred most frequently and are those to which the procedures apply.

Aperture antennas constitute the other large category of antenna names recorded in the GMF. Aperture antennas generally have high gain (greater than 18 dBi) and are often used at frequencies above 1.2 GHz. A variety of aperture antennas are employed in Government radiocommunication systems.

Aperture antennas are used by both radar and communication systems. These systems may be both mobile and fixed. Aperture antennas are also used by the earth stations for transmission of signals to satellites. The geometries of aperture antennas can be either circular or rectangular. TABLE 3-1 lists aperture antennas represented in the GMF; the asterisks reflect to those which the procedures apply.

## SECTION 4

### ANALYSIS

#### ANALYSIS PROCEDURES

Detailed information on antennas often necessary for an accurate treatment of their near field is not generally available. In addition, the variety of antenna geometries used in these systems make it impractical to custom design a model for the near field analysis of each antenna configuration. To achieve a general procedure, accuracy had to be compromised to some extent. A procedure which yields conservative results without placing undue restrictions on the use of systems was developed. Moreover, the procedure had to be simple and amenable to hand calculations for fast and repeated use.

It was assumed that the data for this procedure are primarily limited to those presently available in the GMF and that which the agencies will continue to provide for system review process. The present data on the antennas for a system furnished by an agency for the purpose of system review are limited to the following items:

1. Antenna name
2. Transmitter power
3. Antenna mainbeam gain
4. First sidelobe levels
5. 3-dB beamwidth(s)
6. Frequency

In carrying out the procedure for the near field analysis of an antenna, if the above data are found to be insufficient, the engineer should request additional data. However, generally the data on the five items listed above are sufficient to use the procedure discussed here, for estimating the near field of antennas.

Approximately 200,000 GMF records extending to 300 GHz were examined and two broad categories, i.e., linear and aperture, were found to be adequate for a simple categorization of the antennas. The results of this categorization are shown in TABLE 3-1 and discussed in Section 3. The repetitious use of an antenna name in a large number of assignments was considered indicative of the wide spread use of that antenna.

Three representative antenna types; a resonant dipole in the linear antenna category, a paraboloidal circular dish reflector and a rectangular reflector in the aperture antenna category were selected to be the basic building blocks for the analysis of antenna near field assessment. The results obtained for these three representative antenna types may be extended to calculate the field intensities for a large number of antennas, using appropriate correction factors. For example, the field intensity of a Yagi or log periodic can be estimated by simply multiplying the field of one dipole by a correction factor. This method of extension is discussed further later in this report.

From a radiation hazard point-of-view transmitters with higher power can produce high levels of field intensities over a large area. According to the GMF, the majority of high power transmitters use aperture antennas. The procedure described here for the aperture antennas is an extension of a method published extensively and used by a number of agencies for estimating the near field intensities of such antennas.

#### COMPUTER MODELS

There are a number of computer models which may be used for calculating near field intensity and far field patterns of antennas. These models were

originally developed for antenna design and EMC analysis. Some of these models often used by both Federal agencies and non-government organizations are Numerical Electromagnetic Code (NEC) developed by the Lawrence Livermore Laboratories under a contract with the U.S. Navy, the General Electromagnetic Code (GMAC) developed by the U.S. Air Force, and the Numerical Electromagnetic Code-Reflector Antenna Code (NEC-REF) developed by the Ohio State University under a contract with the U.S. Navy and the U.S. Army. These models represent state-of-the-art technology and very carefully take into account the electrical geometry of any desired antenna in the analysis. Therefore, these models yield accurate results when they are used correctly. The price for this accuracy and rigor, however, is the increase in complexity, the extensive input data, and the training that users of the model must receive in advance. These requirements have hindered the widespread application of these models. The complexity and the extensive input data required has always precluded the use of these models by NTIA in assessing the near field intensity of a large variety of antennas used in Government systems. In addition, a majority of the Government agencies that do not normally request that kind of data during procurement may not be able to utilize these models readily in every radiation hazard analysis. Hence, the requirement for a simple and less demanding procedure applicable to radiation hazard analysis is evident. These models are described as a survey of literature on antenna analysis in partial fulfillment of the objectives of the task covered by this report. In addition, the NEC model was used in developing a simple and more practical computational procedures.

These simplified procedures, although lacking rigor, are useful in estimating the field intensity of a majority of the antennas presently used. This first order conservative estimate, is deemed sufficient for the NTIA in alerting user agencies to the potential hazard of a system during the development stages of a system. Additional analysis may be carried out independently by each agency at its discretion to ensure compliance with the radiation hazard criteria.

A discussion of the complex computer models noted above including their advantages and limitations is given in this section. Some of the Government

agencies may use these models in their radiation hazard assessments. The calculation procedures explained here are based on the existing practices common to the Government and non-Government organizations. The procedure may not be directly applicable to some of the antennas not widely used in which case care should be exercised in extending the procedures to cover the analysis of such antennas. In rare cases where the procedures fail to give satisfactory results, measurement may be recommended. The procedure for near field measurement is extensive and is not discussed in this report. A more extensive effort to develop a practical measurement procedure will be required at a later date. However, the application of any measurement procedure is costly and time consuming. Hence, it is advisable to resort to measurement only when it is necessary.

#### Numerical Electromagnetic Code -- Reflector Antenna

The Numerical Electromagnetic Code -- Reflector Antenna Code (NEC-REF) has the capability for calculating both near and far fields of reflector antennas with paraboloidal surfaces. The algorithm of the code is based on a combination of Geometrical Theory of Diffraction (GTD) and Aperture Integration (AI) techniques. These techniques have been widely published and the papers by Rudduck (Rudduck, 1979) and Burnside (Burnside, 1980) are among the many references. AI, also known as the aperture field method, is used in this algorithm to calculate the main beam and near sidelobe pattern of an antenna whereas the field for larger angles from the axis and the back side of the antenna is calculated using the GTD technique. For calculating the field intensities in the regions very close to an antenna the algorithm makes use of the GTD technique. Both the GTD and AI techniques as used in the NEC-REF code have a basic limitation on the minimum-size reflector that can be modeled. By comparison with the exact solution for the case of a circular disk, the code has been shown to be reasonably accurate for reflector diameters as small as three wavelengths (Lee, 1980). Practical aperture antennas with parabolic surfaces are generally larger than three wavelengths.

Hence the techniques are useful for determining the field intensities of



the majority of the parabolic reflector antennas used by the Government agencies and their systems. However, the code is complex and does not provide a general scheme for calculating the near field intensities of any aperture antennas. The practical limitations of the NEC-REF code can be summarized as follows:

1. The reflector surface must be paraboloidal.
2. The feed must be located near the focus. The effect of defocusing is included by calculating the phase change caused by path length perturbation.
3. The grid size used for aperture integration must be chosen sufficiently small to give a good representation of the aperture field distribution.
4. Array variables associated with the rim data, the principal grid, the feed pattern and the output pattern must be given sufficient dimensions for the required input data. Similar restrictions apply to the dimensions of struts and plates.
5. The feed assembly plate must be located inside the projected aperture. The variation of the incident field (aperture field) over the cross section of the feed blockage plate should be small because the feed blockage model assumes a uniform plane wave with field level that matches the on axis aperture field.
6. The strut diameters should be no more than 10 wavelengths. The source of strut scattering is the geometrical optics fields from the reflector surface. Other strut scattering mechanisms, such as direct feed scattering from the strut, are not modeled.
7. The GTD source model must be used to calculate the effects of near field obstacles on the near field patterns of reflector antennas. The effects of near field obstacles are neglected in the AI region of the reflector antenna near field. Consequently, an obstacle cannot protrude into the projected aperture for near field calculations.
8. Reflector to linear coupling with near field obstacles can be calculated with the GTD source model, but not with the YSUM source model. YSUM was developed using an aperture integration algorithm.

#### Numerical Electromagnetic Code (NEC)

The NEC is a user-oriented code designed for the analysis of radiating or

scattering wires and surfaces. The NEC algorithm is based on the method of moments [Harrington 1967, and 1968]. Moment methods have been used to treat a wide variety of radiation and scattering problems and have also been applied to a number of problems in electromagnetic compatibility. In the moment method, the computation of near fields proceeds directly from a general formulation applicable to any geometry. However, specific solution for any antenna is accomplished by a fairly detailed knowledge of the antenna physical geometry. NEC computations for any antenna are generally carried out in two steps. First, the program computes the current distribution on the radiating surfaces of the antenna. This distribution always satisfies the necessary boundary conditions and hence it is a valid and realizable solution to the Maxwell's equation. Then the radiation in the far field and near field regions of the antenna is treated by the program using the classical approach. The calculation of the current distribution sometimes referred to as "distribution" on the antenna is essential to the computation of the near field intensities of antennas. In the absence of such calculation, solution to any radiating antenna can be obtained by assuming a realizable distribution for the antennas.

The NEC program is used to model a variety of structures, perfect or imperfect conductors, placed over a ground plane that may either be perfect or lossy. The excitation can be a voltage or current source. A plane-wave with linear or elliptical polarization may also be modeled by the NEC program. The user's manual prepared by Burke (Burke and Poggio, 1981) gives a detailed description of the code and has easy-to-follow instructions for preparing the input data required.

NEC-2, the most recent version of NEC, is the latest in a long line of modifications that have been made to the program in the last decade. There are a number of options available in the application of the NEC for the analysis of wire antennas. There are also some limitations that impede a rigorous solution to these problems. Some of the advantages, as well as the disadvantages, of the NEC-2 as applied to the analysis of linear antennas should be noted in order to identify the role of the model in radiation hazard analysis.

A major disadvantage of the NEC-2 (or simply NEC) is the inability to take into account the effects of the terrain under, or in the vicinity of, the antenna. The ground under the antenna, as far as NEC is concerned, is always flat. A flat ground plane is applicable to locations where roughness of the ground (hills and valleys) represents no serious scattering problems and has no shadow regions. The nearby terrain often produces anomalies that make it difficult to achieve a good agreement between the calculated or measured data.

Another limitation of the NEC program, which is common in any type of numerical analysis, is that the antenna size related to the matrix order in the solution is limited by the size of the memory available in the computer. This limitation determines the extent to which the detailed structure of an antenna can be modeled. Since each antenna is modeled by a collection of wire segments, the larger the antenna, the more segments are required. Note that each segment is represented by an element of the impedance matrix in the equation  $[V] = [Z] \times [I]$  where  $V_i$ , an element of  $[V]$ , represents generalized voltage and  $Z_{ij}$ , an element of  $[Z]$ , is generalized impedance. The column matrix  $[I]$  represents the current distribution on the antenna. The elements of  $[I]$  are complex and require two locations in the memory storage of the computer. For example, if a wire antenna is represented by 100 segments, the impedance matrix is of the order 100, and 20,000 memory locations are required in order to store the matrix. The larger the matrix, the more Central Processing Unit (CPU) time is needed to carry out the computation. Note that the two major limitations discussed above for the analysis of linear antennas are solely for the application of NEC in the analysis of these antennas and should not be considered as general limitations to the matrix methods or even the NEC program. There is a large number of electromagnetic problems that may be solved rigorously using the NEC program.

The advantage of the NEC in treating the near or far field of a linear antenna is its flexibility in taking into account the geometry of the other antenna, or antenna-like structures, in the neighborhood of the antenna being analyzed. Hence, one can readily model any bends or orientation of a wire antenna as well as its support structures. In addition, the NEC program takes

into account the effects of the imperfect ground under the antenna. The length of the segment discussed above is a function of wavelength. Usually, a segment can be as long as 0.1 wavelengths. Therefore, the longer the wavelength, the larger the antenna size that can be analyzed using the NEC program. At low frequencies, the NEC program can handle large size antennas. This is advantageous and allows reasonable computation time.

The NEC model presently implemented on the NTIA computer has a graphics capability. The graphics part of the program may be used in demand mode to obtain a plot of the antenna geometry modeled by the data card and this capability helps to verify that the data cards describe the intended geometry. The graphics capability may also be used to plot the calculated results produced by the program. The near field capability of the model can determine electric and magnetic field intensities for any given geometry at any location above the ground in front of the antenna. The contour plot capability of the model, which is presently available only on the NTIA version of the NEC, can produce contours of the near field for many applications such as radiation hazard analyses.

The NEC has been validated by the NTIA [Farrar, 1985] and a number of other agencies. The validation results indicate that for the majority of analysis the NEC model may be used to obtain results with acceptable engineering accuracy.

Despite the advantages, practical consideration associated with the data bases available to the NTIA and to some of the agencies, prevent the use of the NEC for day-to-day radiation hazard assessment of Government systems. However, the NEC model may be used to develop a simple procedure for calculating the near field intensities of linear antennas. In this approach, there is a trade-off between simplicity and accuracy. Generally, the simpler the procedure, the more applicable it will be to a large variety of antennas included in the category of linear antennas, and the less accurate the results may be. This is more evident when the procedure is extended beyond its range through the use of analogy and inference.

The NEC program was used to validate the simple procedure described here for calculating near fields of some types of linear antennas more often used

by Government systems. A more detailed description of this approach is given later in this report.

#### SIMPLIFIED MODELS FOR NEAR FIELD CALCULATIONS

This section includes a discussion of simple analytical procedures developed for calculating the field intensities for aperture and some of the linear antennas. The procedures are general and may be applied to a large variety of antenna and essentially require no additional data base or information other than what is generally made available by the agencies prior to a system review. Moreover, the procedures are quite simple and easy to use. They require no special training and may be used in assessing the field intensity in the near field of antennas.

#### Aperture Antennas

A literature search conducted during this effort indicated that essentially the same methods are now being used by the U.S. Navy, Air Force, and the Army for calculating the field intensities of aperture antennas. A discussion of the calculation procedure used by the NAVY, Air Force and the Army is given in NAVSEA-OP-3565/NAVAIR-16-1-529, T.O. 312-10-4, and (Army) FM1-490-30, respectively. The method of calculation adopted by these agencies is based on the earlier analysis proposed by Hanson [Bickmore, R. W., and Hansen, R. C., 1959] Hansen's analysis was later extended by [Farrar, A. and Adams, A. 1980]. This analysis was based on several theoretical aperture distribution functions given by [Silver, 1949]. The results of such analyses are applicable only to the calculation of field intensities along the main axis of aperture antennas.

The procedure for the near field calculation of aperture antennas discussed here is a refined version of the techniques using by the agencies noted above as was explained in an earlier paper [Farrar, 1980]. The calculation procedure for an aperture was developed using the idea of first

calculating the power density at a distance of  $2D^2/\lambda$  where D is the largest dimension of the aperture. The near field power density for the aperture was then calculated by multiplying the far field power density by a correction factor. The correction factor for each aperture is a function of the aperture distribution, the ratio of  $D/\lambda$  and the shape of the antenna as to whether it is circular or rectangular. A discussion of the development leading to the correction factors for both circular and rectangular apertures will now be given. In the analysis given here, the effect of the feed, struts, and other structural elements has not been taken into account.

Correction Factors for Circular Apertures. Circular apertures may be designed using a variety of distribution function. A general distribution function suggested by Silver [Silver, 1949] and used in the development of techniques adopted by the agencies noted above is of the form:

$$f(\rho) = (1-\rho^2)^n \quad 0 < \rho < 1 \quad (4-1)$$

where  $\rho$  is a variable normalized to the aperture radius R. There are a number of other distribution functions used in the literature [Skolnik, 1970]. These functions have been used for far field calculations and generally do not yield closed form solutions for the near field calculations. The distribution given in Equation 4-1 was used here for simplicity and to maintain conformity with the techniques adopted by some of the Government agencies. Relative to some other distribution function, Equation 4-1 yields more conservative results. The exponent  $n$  in Equation (4-1) is generally assumed to be an integer greater than zero. In practice,  $n$  is a number greater than zero and less than 5. Sidelobe levels, especially the first, and the beamwidth of the antenna vary with the value of  $n$ . Hence, knowing these properties of far field pattern one can assess the value of  $n$  in Equation (4-1). In this way, the aperture function may be carefully determined. The relationships among the parameter  $n$ , the sidelobe level, and the beamwidth will be discussed later in this section.

For  $n = 0$ , the distribution is uniform and the expression for on-axis near field will be

$$P(x) = | 1 - \text{Exp}(j\alpha) |^2$$

where

$$\alpha = 4\pi D_\lambda^2 [x - \sqrt{x^2 + 1/(16 D_\lambda^2)}]$$

$$D_\lambda = 2R/\lambda$$

$$x = z\lambda/2D^2 = \text{normalized on-axis distance}$$

Using the aperture distribution in Equation 4-1, the expression for the on-axis near field may be derived [Farrar, 1980] is

$$P(x) = \left| 1 - \frac{nI}{\beta^n} e^J \right|^2 \quad n > 0 \quad (4-2)$$

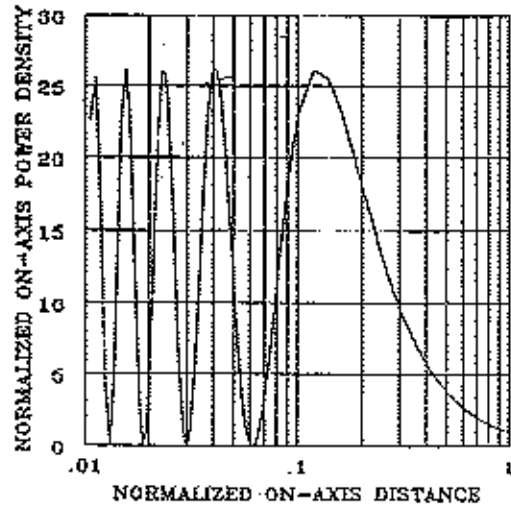
where  $I = \int_0^\beta Y^{n-1} e^{jY} dY$

$$\beta = \pi / (2 \sqrt{16x^2 + 1/D_\lambda^2})$$

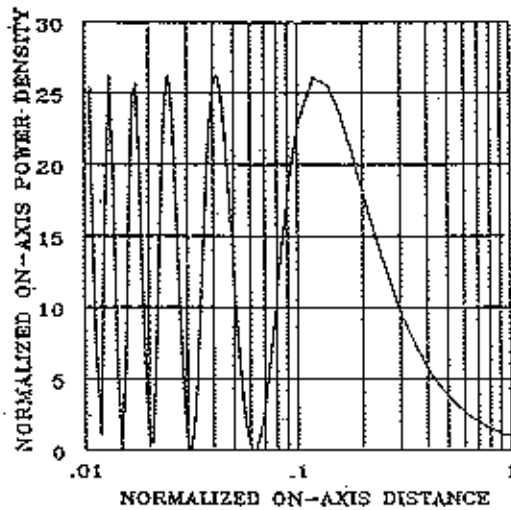
By definition, the correction factor is the ratio of the power density in the near field to the power density at a distance of  $2D^2/\lambda$  along the antenna axis. Mathematically the near field correction factor may be written as

$$\text{Correction Factor} = \text{normalized on-axis power density} = P(x)/P(2D^2/\lambda) \quad (4-3)$$

A computer program was prepared to evaluate the expression given in Equation (4-3) for different values of  $n$  ranging from 0 to 3. The results of such calculations for some typical values of  $D/\lambda$  are shown in Figures (4-1) to (4-3).



(a)



(b)

Figure 4-1. Correction factor vs. on-axis distance normalized to  $2D^2/\lambda$  for a circular aperture with uniform distribution, (a)  $D/\lambda = 20$ , (b)  $D/\lambda = 40$ .



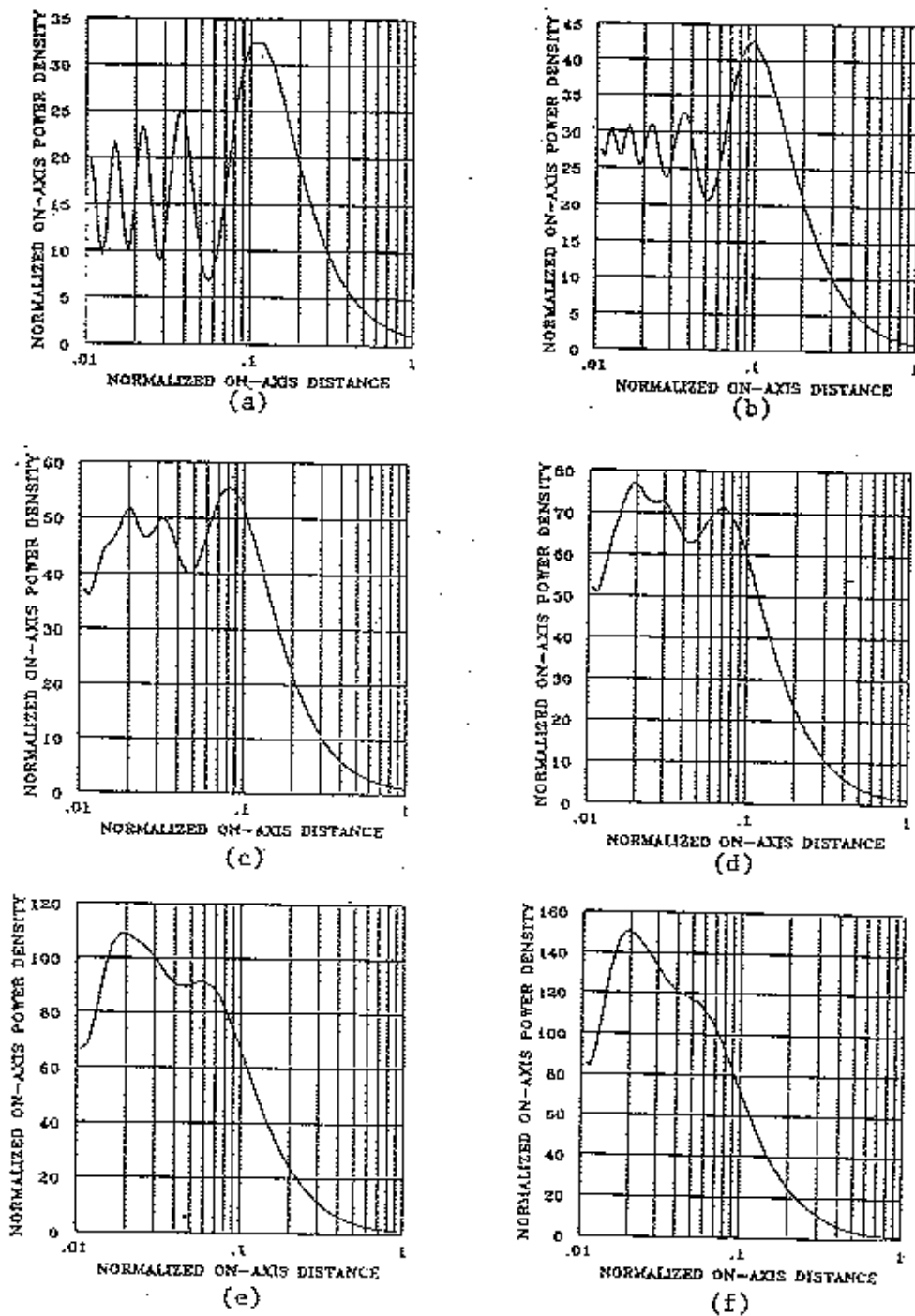
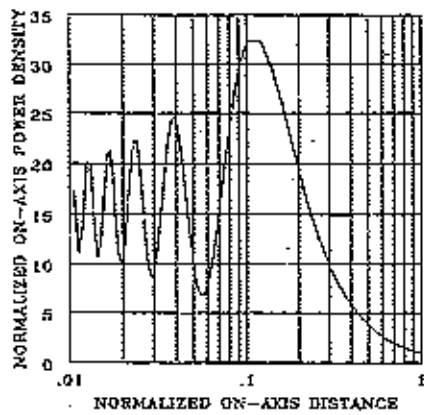
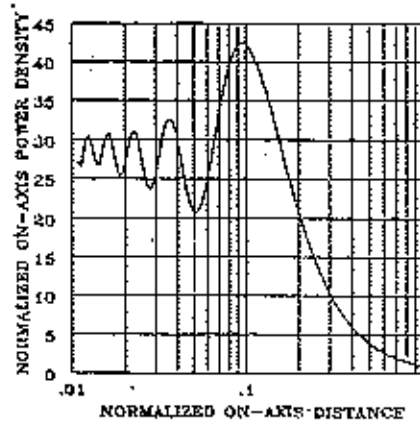


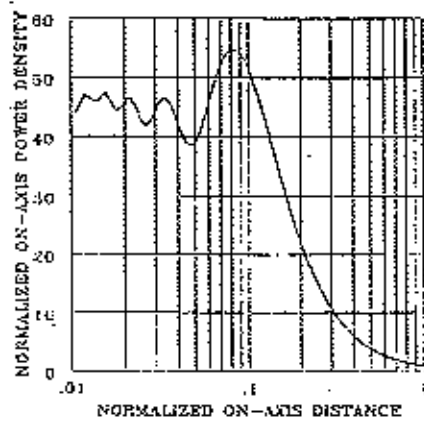
Figure 4-2. Correction factor vs. on-axis distance normalized to  $2D^2/\lambda$  for circular apertures with tapered distributions ( $D/\lambda=20$ ), (a)  $n=0.5$ , (b)  $n=1.0$ , (c)  $n=1.5$ , (d)  $n=2.0$ , (e)  $n=2.5$ , (f)  $n=3.0$ .



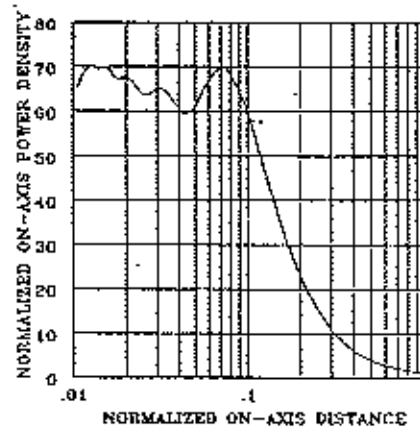
(a)



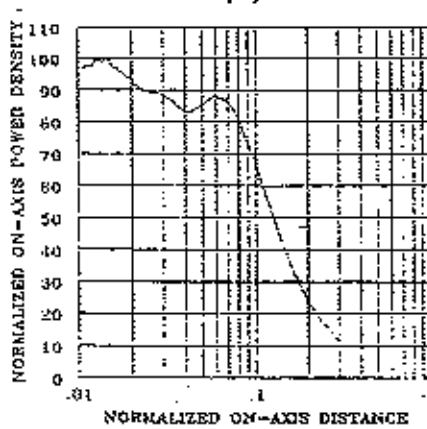
(b)



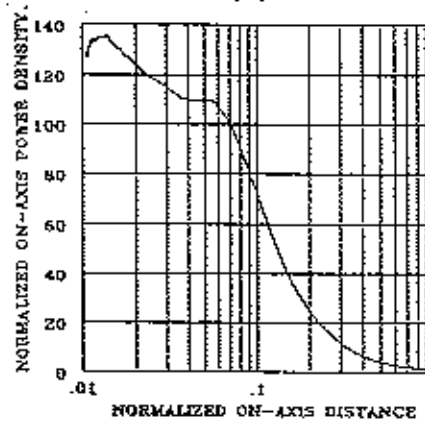
(c)



(d)



(e)



(f)

Figure 4-3. Correction factor vs on-axis distance normalized to  $2D^2/\lambda$  for circular apertures with tapered distributions ( $D/\lambda=40$ ), (a)  $n=0.5$ , (b)  $n=1.0$ , (c)  $n=1.5$ , (d)  $n=2.0$ , (e)  $n=2.5$ , (f)  $n=3.0$ .

Note that for a  $n < 1.5$ , the value of correction factor (CF) in the regions close to the antenna oscillates rapidly with  $x$ . For radiation hazard assessment, the maximum correction factor is of interest. To facilitate such analysis, the data in Figures (4-1a) and (4-2) were plotted in Figure (4-4a) and the data in Figures (4-1b) and (4-3) were plotted in Figure (4-4b). The data in Figures (4-4a) and (4-4b) are conservative and are furnished for easy reference only.

It is noteworthy that the Federal Communications Commission (FCC) has accepted a simplified formula for calculating the near field intensities of aperture antennas (OST Bulletin No. 65, 1985). This formula was derived using the value for maximum correction factor of 26 shown in Figure 4-1, and it may be used primarily to calculate the maximum field intensity for circular apertures having uniform distribution.

Relationships Between  $n$  and Far Field Characteristics. (Circular Apertures) For circular apertures, the dependency of the sidelobe levels and beamwidth of an antenna on the parameter  $n$  in Equation (4-1) may be determined using the far field expression developed by Silver [Silver, 1949]. The far field expression developed by Silver utilizing the distribution function given in Equation (4-1) is given by

$$E_n(u) = 2\pi R^2 \int_0^1 (1-p^2)^n J_0(up) p dp \quad (4-4)$$

*correction factor*

where  $u = \pi D \sin \theta / \lambda$

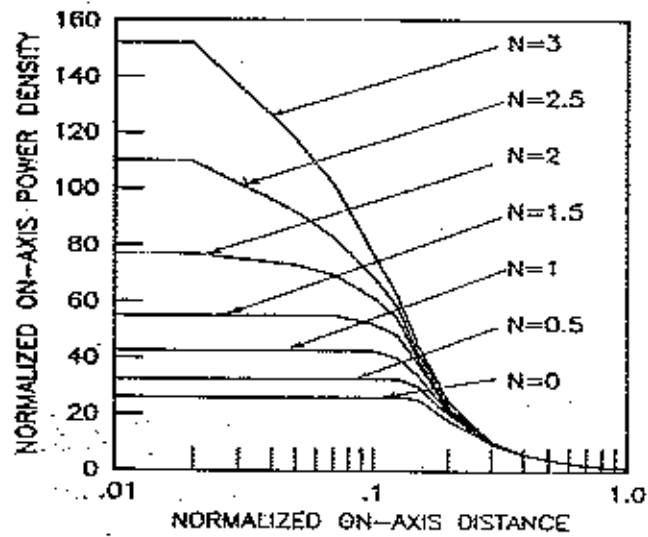
$\lambda$  = Wavelength

$D$  = Diameter of aperture

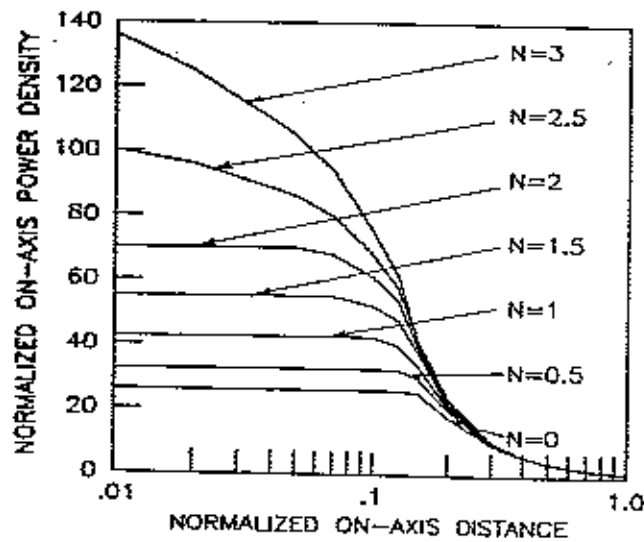
$J_0$  = Bessel function of zero order

In Equation (4-1) if  $n$  is an integer the integration with respect to  $p$  yields the closed form solution

$$E_n(u) = \pi R^2 A_{n+1}(u) / n+1 \quad (4-5)$$



(a)



(b)

Figure 4-4. Maximum correction factor vs. on-axis distance normalized to  $2D^2/\lambda$  for circular apertures, (a)  $D/\lambda = 20$ , (b)  $D/\lambda = 40$ .

where the functions  $J_n$  are available in tabular form. However, when  $n$  is not an integer the integration may be performed by expanding the Bessel function in an infinite series and integrating the series term-by-term.

The results may be written as

$$g_n(u) = \pi R^2 \sum_{k=0}^{\infty} \frac{(-1)^k (u/2)^{2k}}{(k!)^2} \int_0^1 y^n (1-y)^k dy \quad (4-6)$$

A computer program was prepared to carry out the calculations indicated by Equation (4-6). The major characteristics of the patterns calculated using Equation (4-4) are summarized in TABLE 4-1.

TABLE 4-1  
FAR-FIELD PATTERN CHARACTERISTICS PRODUCED BY A  
DISTRIBUTION  $(1-p^2)^n$  OVER A CIRCULAR APERTURE

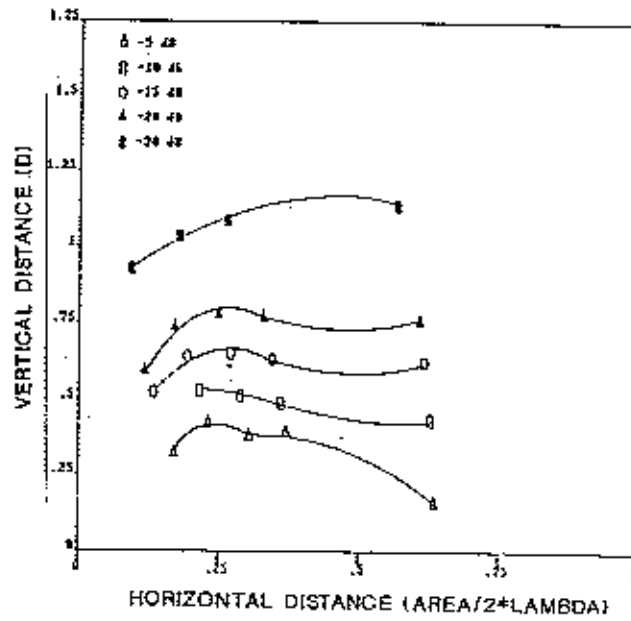
$n$	Half-Power Beamwidth (radian)	Position of 1st Zero (radian)	First Sidelobe dB Below Peak Intensity
0.0	1.02 $\lambda/D$	$\arcsin(1.21 \lambda/D)$	17.5
0.2	1.08 $\lambda/D$	$\arcsin(1.27 \lambda/D)$	19.1
0.5	1.15 $\lambda/D$	$\arcsin(1.43 \lambda/D)$	21.3
0.75	1.21 $\lambda/D$	$\arcsin(1.53 \lambda/D)$	23.0
1.0	1.27 $\lambda/D$	$\arcsin(1.62 \lambda/D)$	24.6
1.2	1.34 $\lambda/D$	$\arcsin(1.72 \lambda/D)$	26.0
1.5	1.40 $\lambda/D$	$\arcsin(1.85 \lambda/D)$	27.7
1.75	1.43 $\lambda/D$	$\arcsin(1.94 \lambda/D)$	29.1
2.0	1.46 $\lambda/D$	$\arcsin(2.04 \lambda/D)$	30.6
2.2	1.53 $\lambda/D$	$\arcsin(2.10 \lambda/D)$	31.7
2.5	1.59 $\lambda/D$	$\arcsin(2.23 \lambda/D)$	33.3
2.75	1.62 $\lambda/D$	$\arcsin(2.32 \lambda/D)$	34.6
3.0	1.66 $\lambda/D$	$\arcsin(2.42 \lambda/D)$	35.9

Clearly, one can determine the parameter  $n$  uniquely from the information given in TABLE 4-1 by knowing half-power beamwidth, position of first zero, or the level of first sidelobe in dB for a circular antenna. Generally, information on the antenna sidelobe level or half-power beamwidth for the antenna may be obtained from NTIA Form 35, prepared by the agency requesting spectrum support.

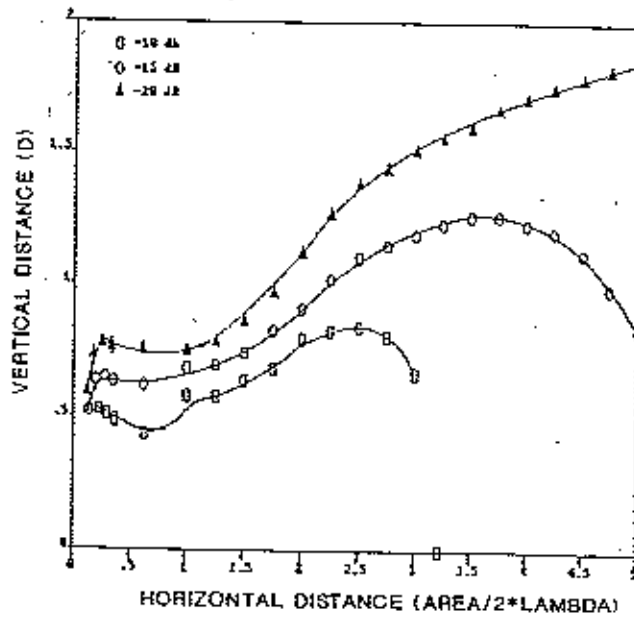
The appropriate correction factor for the antenna may now be obtained from the data in Figure 4-1 to 4-3 after the parameter  $n$  has been determined in the manner described above. This calculation procedure is clarified further later in this section through an example or sample calculations.

Off-Axis Power Density For Circular Apertures: The discussion on circular aperture so far was limited to the treatment of on-axis near field. In practice, these antennas are placed on towers and knowledge of off-axis power density may be essential in assessing the compliance of the radiation from such an antenna on the surface of the earth.

Data for the off-axis power density of the aperture antennas is rather rare, however limited information on circular apertures with uniform distribution is available [ITT, 1975]. Hansen has presented data for circular apertures with uniform and Taylor distribution [Hansen, 1964]. The data in the ITT Handbook was extended using the information developed by Hansen. The results of this effort are shown in Figures 4-5. Note that the distribution of power in the regions close to the antenna as shown in Figure 4-5 varies with distance from the antenna. The distance on horizontal axis in Figure 4-5 is in the unit of aperture area/ $2\lambda$  and the vertical axis shows the distance from the antenna in the unit of antenna diameter. Each curve in Figure 4-5 shows the level of power density below that calculated for on-axis locations of the antenna. The data in Figure 4-5 pertains to uniform distribution only. Off-axis analysis for tapered distribution of circular antennas was not included in the analysis given here.



(a)



(b)

Figure 4-5. Data for off-axis calculation of power density, (a) regions close to the antenna, (b) regions further away from antenna.

Correction Factors for Rectangular Apertures. Rectangular apertures are used in a large number of the Government telecommunications systems. Square apertures may be treated as a special case of the rectangular apertures. Examples of rectangular apertures include horn antennas, some grid or solid type reflector antennas, and passive reflectors.

The relationships useful in calculating the field intensities in front of a rectangular aperture with length and width of  $2a$  and  $2b$ , respectively, were derived using the distribution functions

$$f(x', y') = \cos^n \frac{\pi x'}{2a} \quad -a \leq x' \leq a \quad (4-7)$$

where  $n = 0, 1, 2, 3$ , and

$$f(x', y') = \left( \cos \frac{\pi x'}{2a} \cos \frac{\pi y'}{2b} \right)^n \quad -b \leq y' \leq b \quad (4-8)$$

where  $n = 1, 2$ .

Note that for  $n = 0$ , the distribution is uniform. The parameter  $n$  affects directly the disposition of the far field characteristics. The dependency of these characteristics on  $n$  may be used to determine the value of  $n$ . The determination of  $n$  is discussed in greater detail later in this section. A comparison of Equation (4-7) with (4-8) shows that in Equation (4-7) the distribution function is cosinusoidal along the  $x$  axis and uniform along the  $y$  axis whereas in Equation (4-8), the distribution is cosinusoidal along both the  $x$  and  $y$  axis.

For this analysis the deciding factor as to whether an aperture is rectangular or circular is based on the antenna rim shape. The shape of any antenna rim may be approximated by a square, a rectangle, or a circle.



The six distribution functions given in Equation (4-7) and (4-8) were used to derive the on-axis near-field relationships given in Table 4-2.

TABLE 4-2  
RELATIONSHIPS FOR ON-AXIS POWER DENSITY CALCULATIONS  
FOR RECTANGULAR APERTURES

ON-AXIS POWER-DENSITY EXPRESSION*	APERTURE DISTRIBUTIONS
$P_{co} =  P ^2$	Uniform
$P_{c1} =  P_1 ^2$	$\cos \pi x' / 2a$
$P_{c2} =  P + P_{2a} ^2$	$\cos^2 \pi x' / 2a$
$P_{c3} =  P_3 + 3P_1 ^2$	$\cos^3 \pi x' / 2a$
$P_{cc1} =  P_{1c} ^2$	$\cos \pi x' / 2a \cos \pi y' / 2b$
$P_{cc2} =  P + P_{2a} + P_{2b} + P_{2cc} ^2$	$\cos^2 \pi x' / 2a \cos^2 \pi y' / 2b$

\* Symbols in this column are defined in Appendix A.

Using the relationships given in Table 4-2, normalized power densities for various distribution functions were calculated. The results of such calculations are given in Figures 4-6 to 4-18.

The determination of the parameter  $n$  applicable to a rectangular aperture is carried out in a manner similar to that described for the circular apertures.

Relationships Between n and Far Field Characteristics. (Rectangular Apertures) To facilitate the analysis of rectangular apertures, the simplified expressions for the Fraunhofer region derived by Silver will be used. So far as the pattern calculation is concerned, we need consider only the factor

$$g_n(\theta, \phi) = \int_{-a}^a \int_{-b}^b f(\xi, \eta) e^{jk \sin \theta (\xi \cos \phi + \eta \sin \phi)} d\xi d\eta \quad (4-9)$$

where

$f(\xi, \eta)$  = distribution function

$2a$  = length of aperture

$2b$  = width of aperture

$k$  = wave number

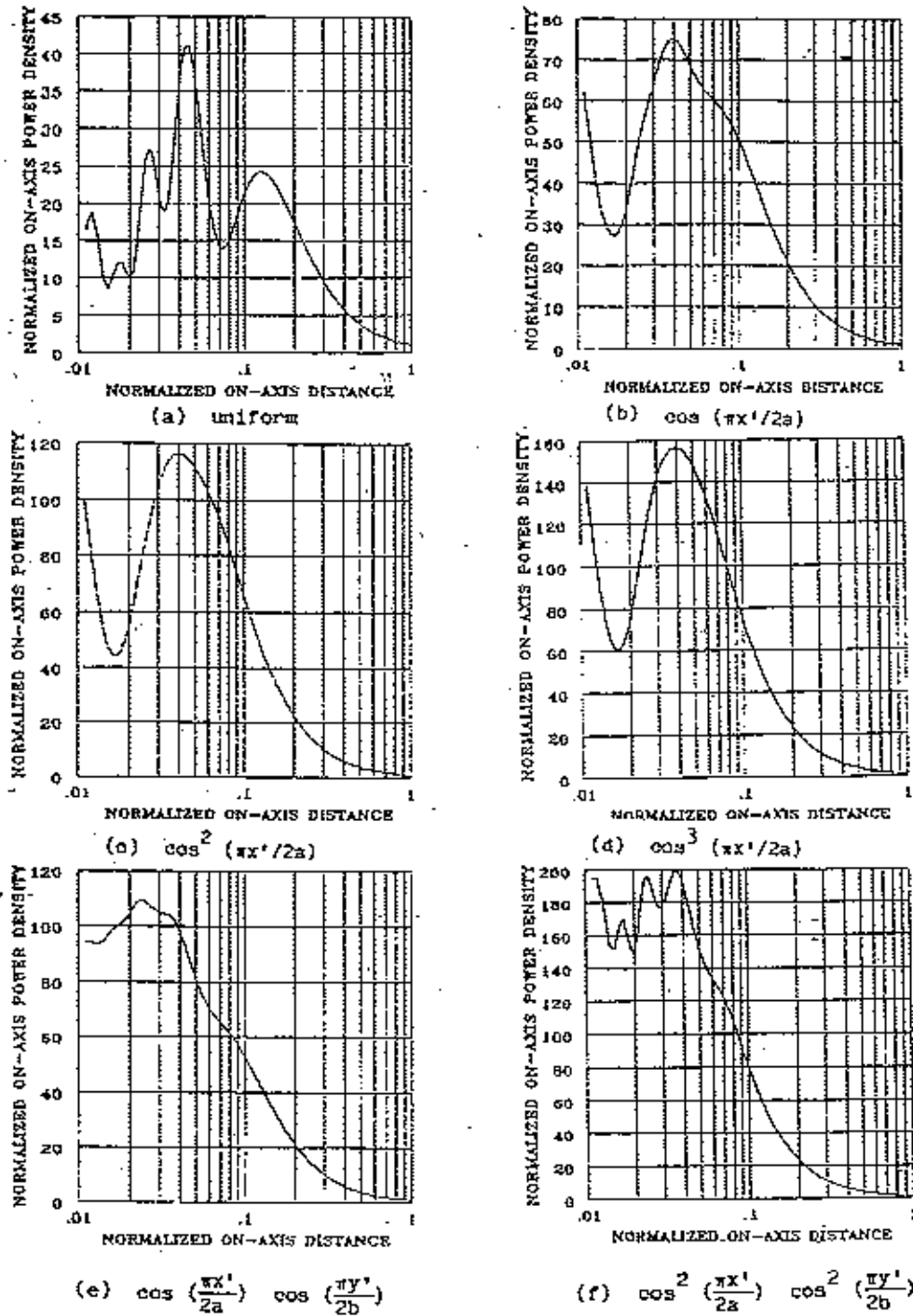
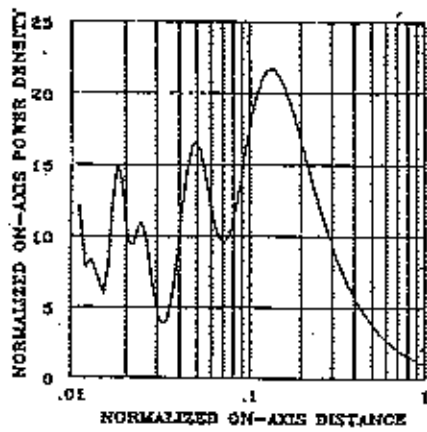
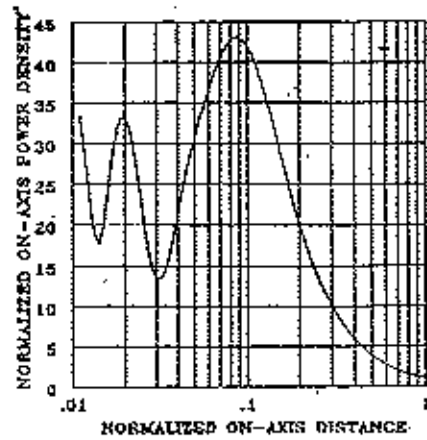


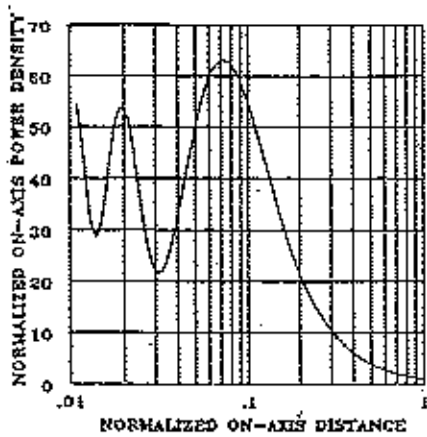
Figure 4-6. Correction factor vs. on-axis distance normalized to  $8a^2/\lambda$  for rectangular aperture with dimensions  $a/\lambda=20$ ,  $b/\lambda=10$ , and different distribution functions.



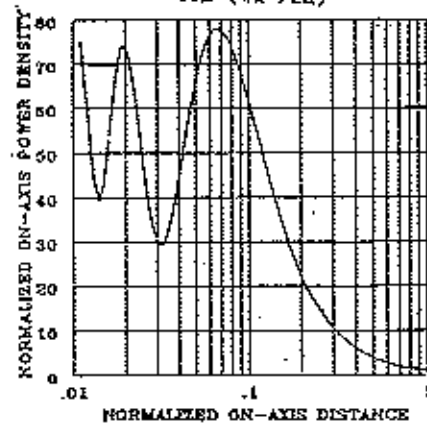
(a) uniform



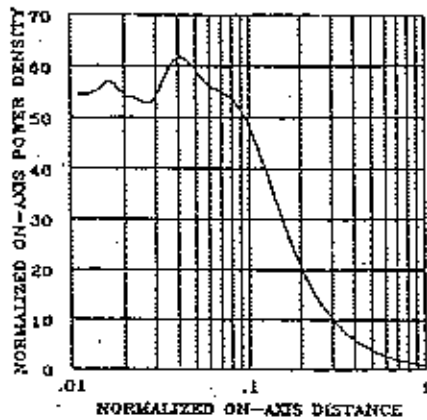
(b)  $\cos(\pi x'/2a)$



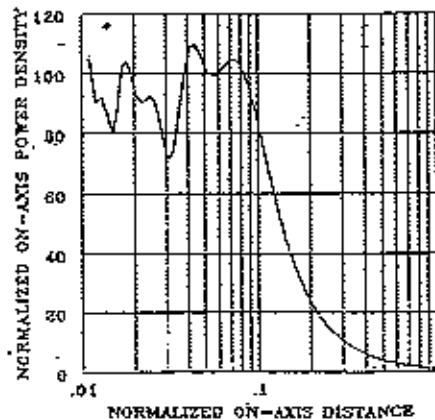
(c)  $\cos^2(\pi x'/2a)$



(d)  $\cos^3(\pi x'/2a)$



(e)  $\cos\left(\frac{\pi x'}{2a}\right) \cos\left(\frac{\pi y'}{2b}\right)$



(f)  $\cos^2\left(\frac{\pi x'}{2a}\right) \cos^2\left(\frac{\pi y'}{2b}\right)$

Figure 4-7. Correction factor vs. on-axis distance normalized to  $8a^2/\lambda$  for rectangular aperture with dimensions  $a/\lambda = 30$ ,  $b/\lambda = 10$ , and different distribution functions.

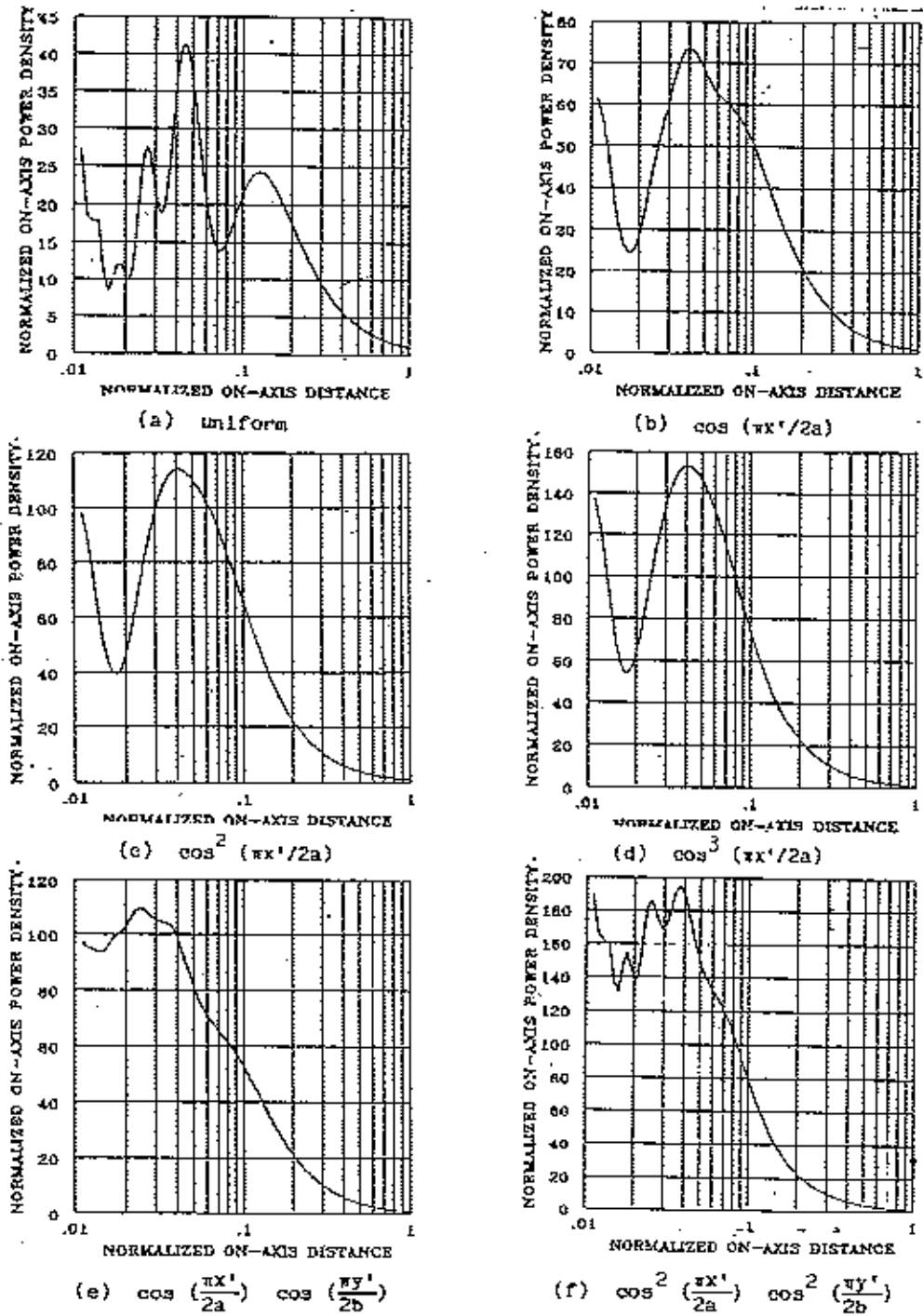
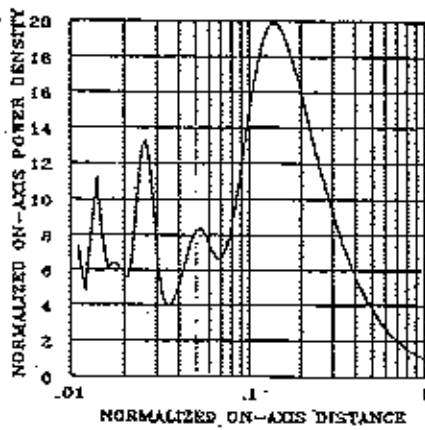
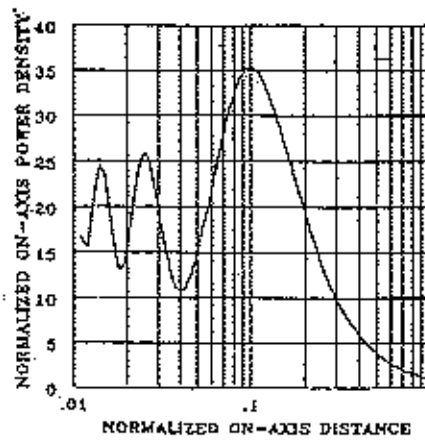


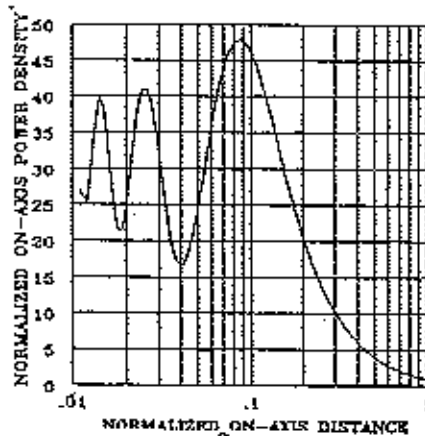
Figure 4-8. Correction factor vs. on-axis distance normalized to  $8a^2/\lambda$  for rectangular aperture with dimensions  $a/\lambda=40$ ,  $b/\lambda=20$ ; and different distribution functions.



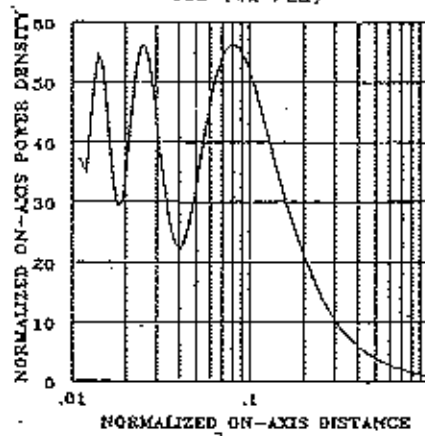
(a) uniform



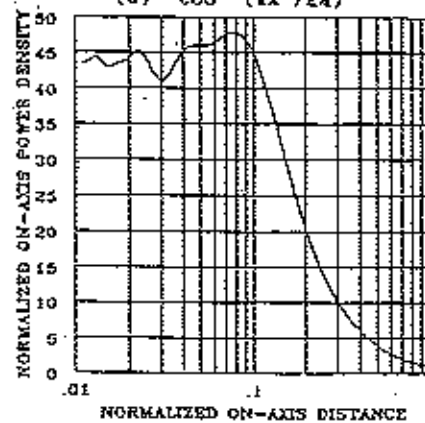
(b)  $\cos(\pi x'/2a)$



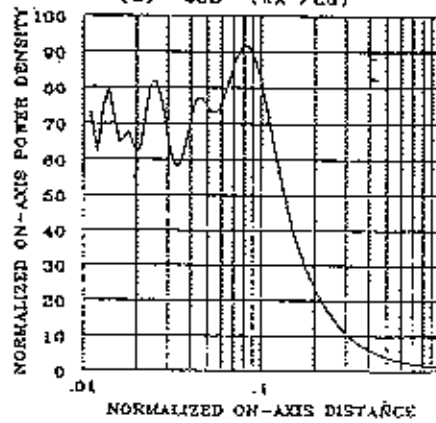
(c)  $\cos^2(\pi x'/2a)$



(d)  $\cos^3(\pi x'/2a)$



(e)  $\cos\left(\frac{\pi x'}{2a}\right) \cos\left(\frac{\pi y'}{2b}\right)$



(f)  $\cos^2\left(\frac{\pi x'}{2a}\right) \cos^2\left(\frac{\pi y'}{2b}\right)$

Figure 4-9. Correction factor vs. on-axis distance normalized to  $8a^2/\lambda$  for rectangular aperture with dimensions  $a/\lambda = 40$ ,  $b/\lambda = 30$ , and different distribution functions.

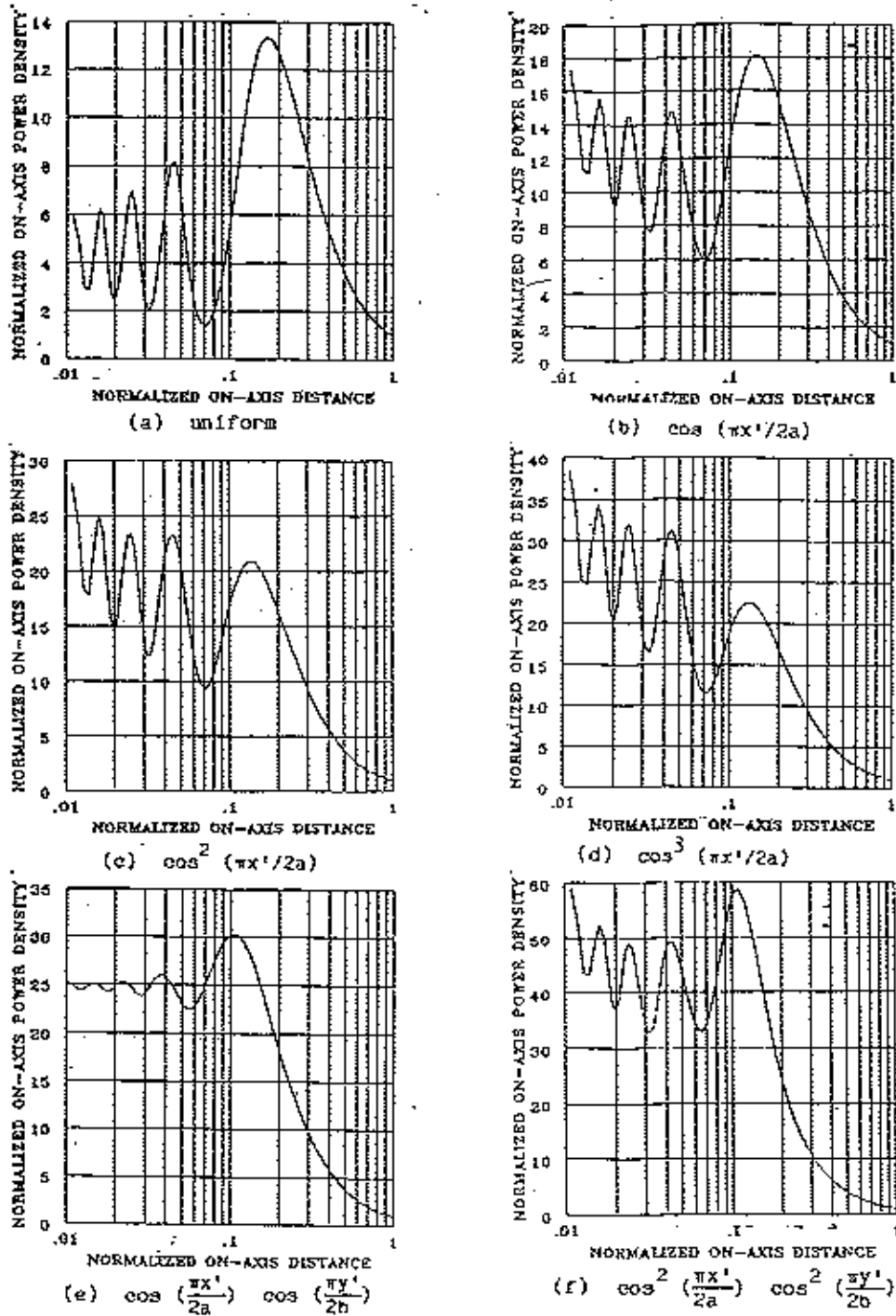


Figure 4-10. Correction factor vs. on-axis distance normalized to  $8a^2/\lambda$  for rectangular aperture with dimensions  $a/\lambda=20$ ,  $b/\lambda=20$ , and different distribution functions.

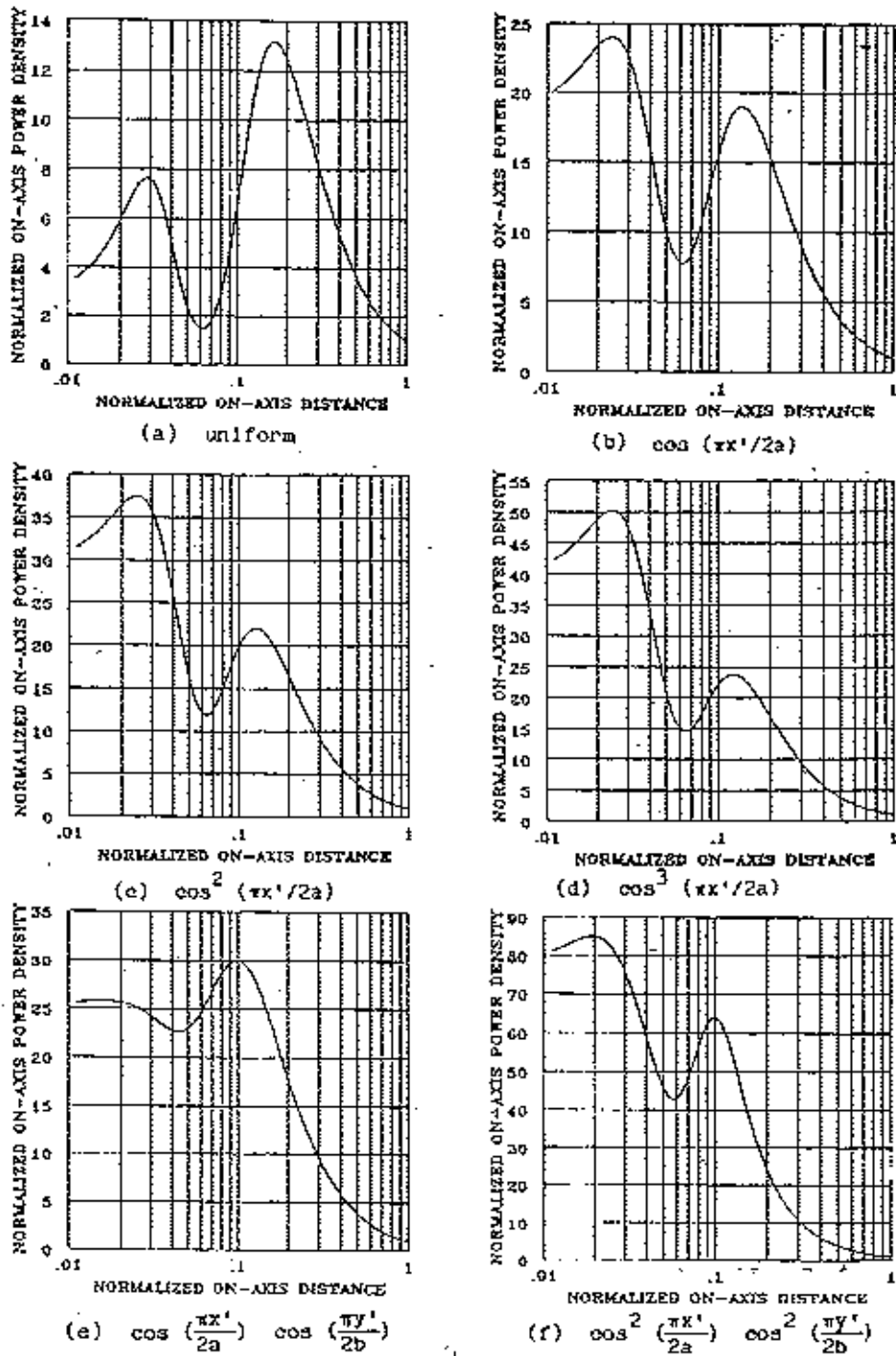


Figure 4-11. Correction factor vs. on-axis distance normalized to  $8a^2/\lambda$  for rectangular aperture with dimensions  $a/\lambda=5$ ,  $b/\lambda=5$ , and different distribution functions.



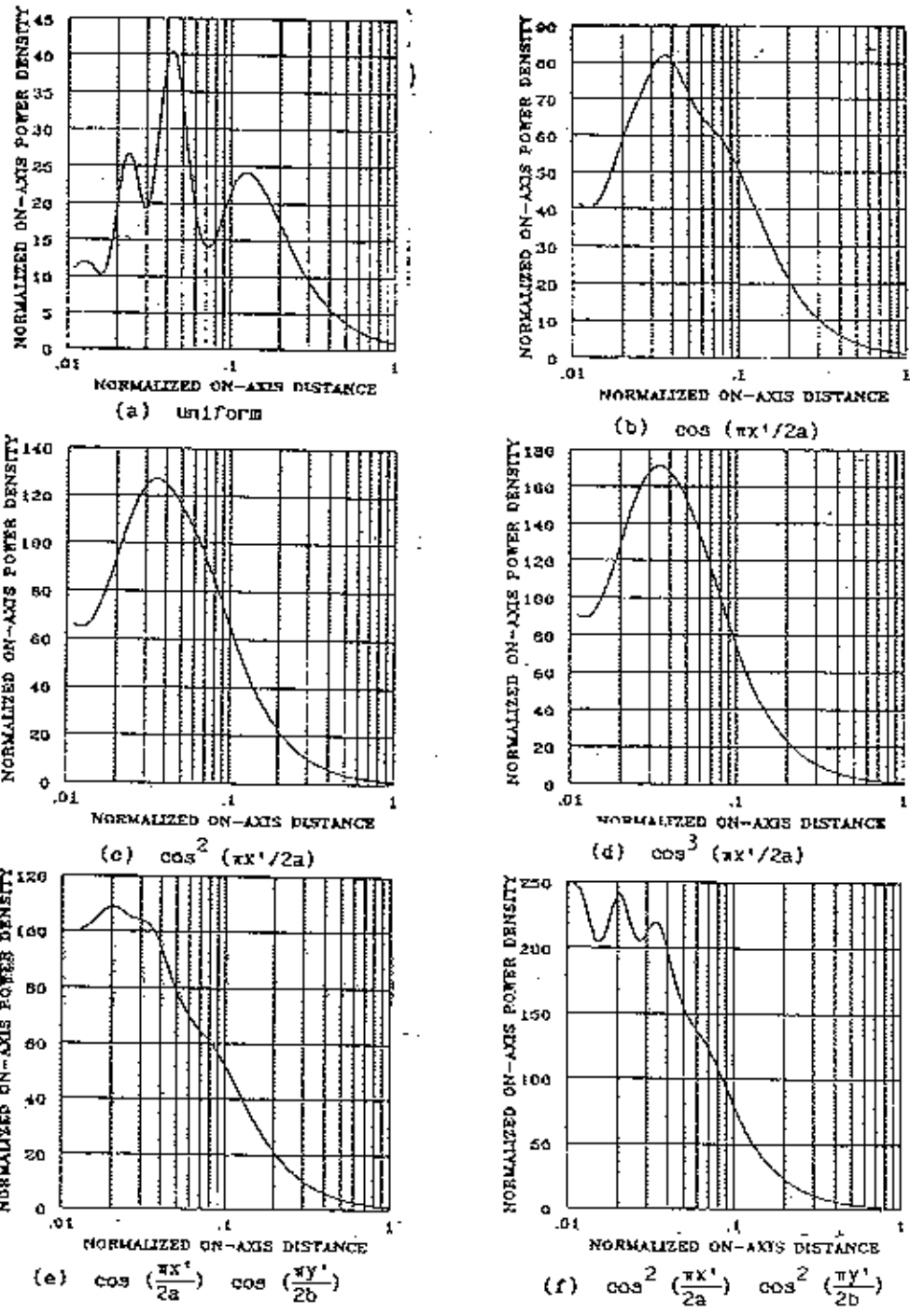


Figure 4-12. Correction factor vs. on-axis distance normalized to  $Ba^2/\lambda$  for rectangular aperture with dimensions  $a/\lambda=10$ ,  $b/\lambda=5$ , and different distribution functions.

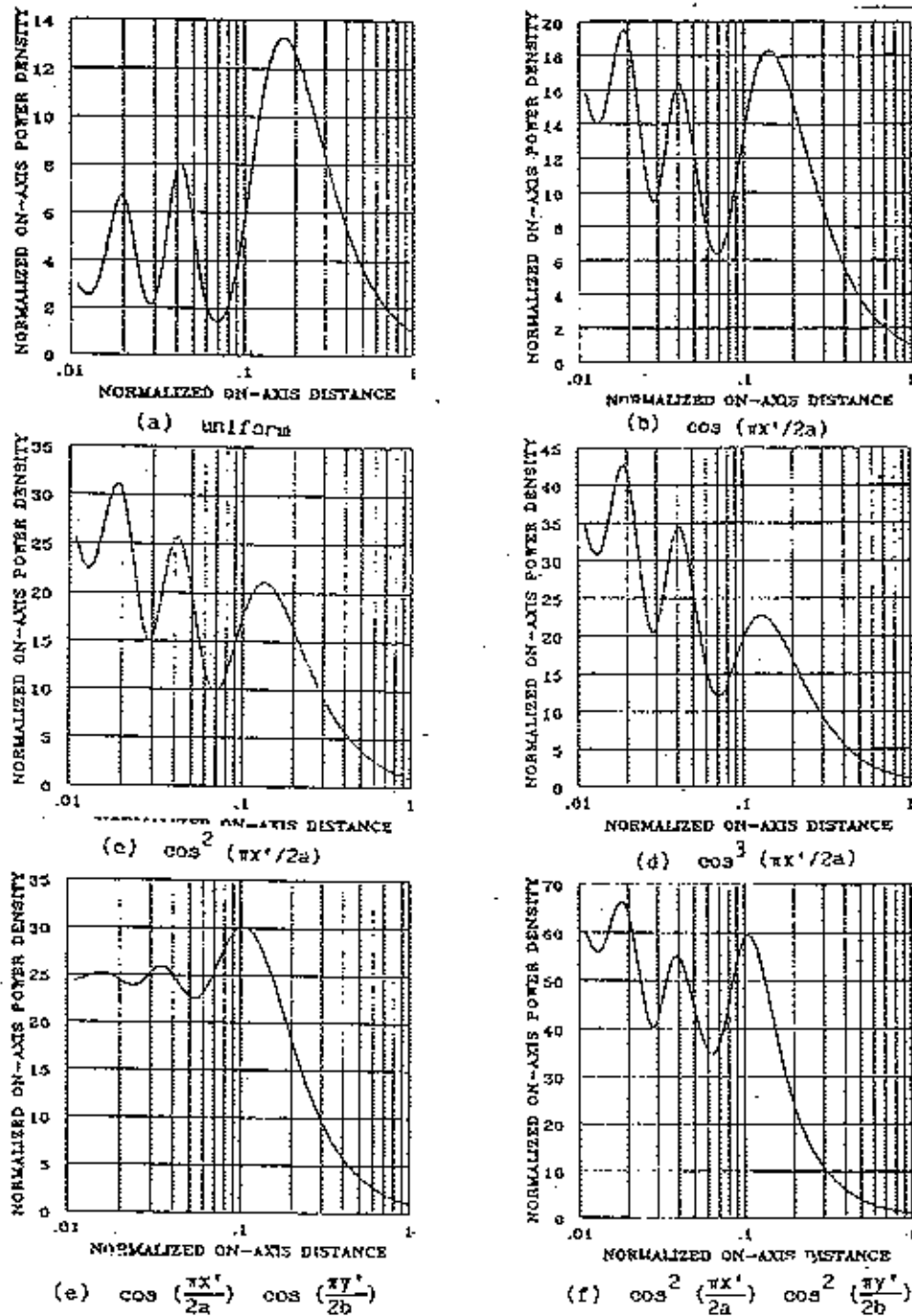
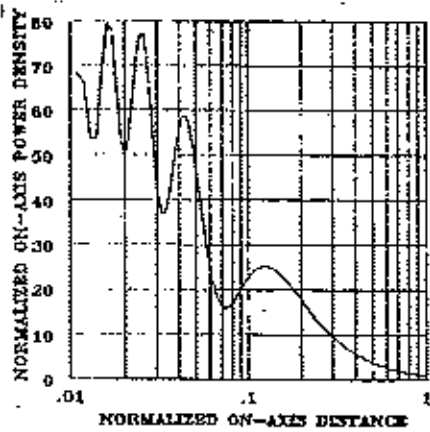
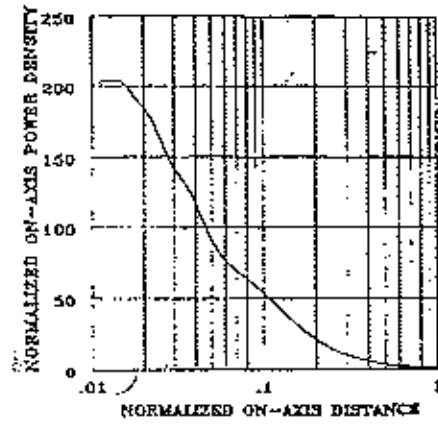


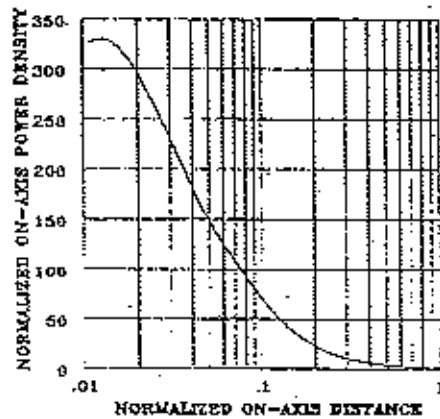
Figure 4-13. Correction factor vs. on-axis distance normalized to  $8a^2/\lambda$  for rectangular aperture with dimensions  $a/\lambda=10$ ,  $b/\lambda=10$ , and different distribution functions.



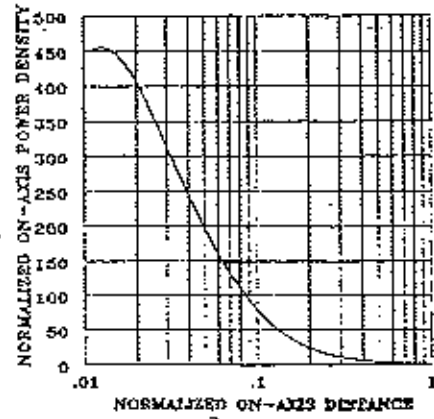
(a) uniform



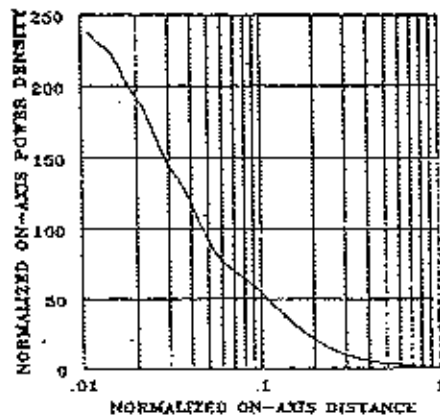
(b)  $\cos(\pi x'/2a)$



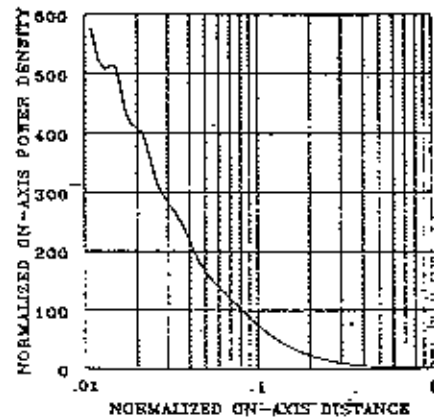
(c)  $\cos^2(\pi x'/2a)$



(d)  $\cos^3(\pi x'/2a)$



(e)  $\cos\left(\frac{\pi x'}{2a}\right) \cos\left(\frac{\pi y'}{2b}\right)$



(f)  $\cos^2\left(\frac{\pi x'}{2a}\right) \cos^2\left(\frac{\pi y'}{2b}\right)$

Figure 4-14. Correction factor vs. on-axis distance normalized to  $8a^2/\lambda$  for rectangular aperture with dimensions  $a/\lambda=15$ ,  $b/\lambda=5$ , and different distribution functions.

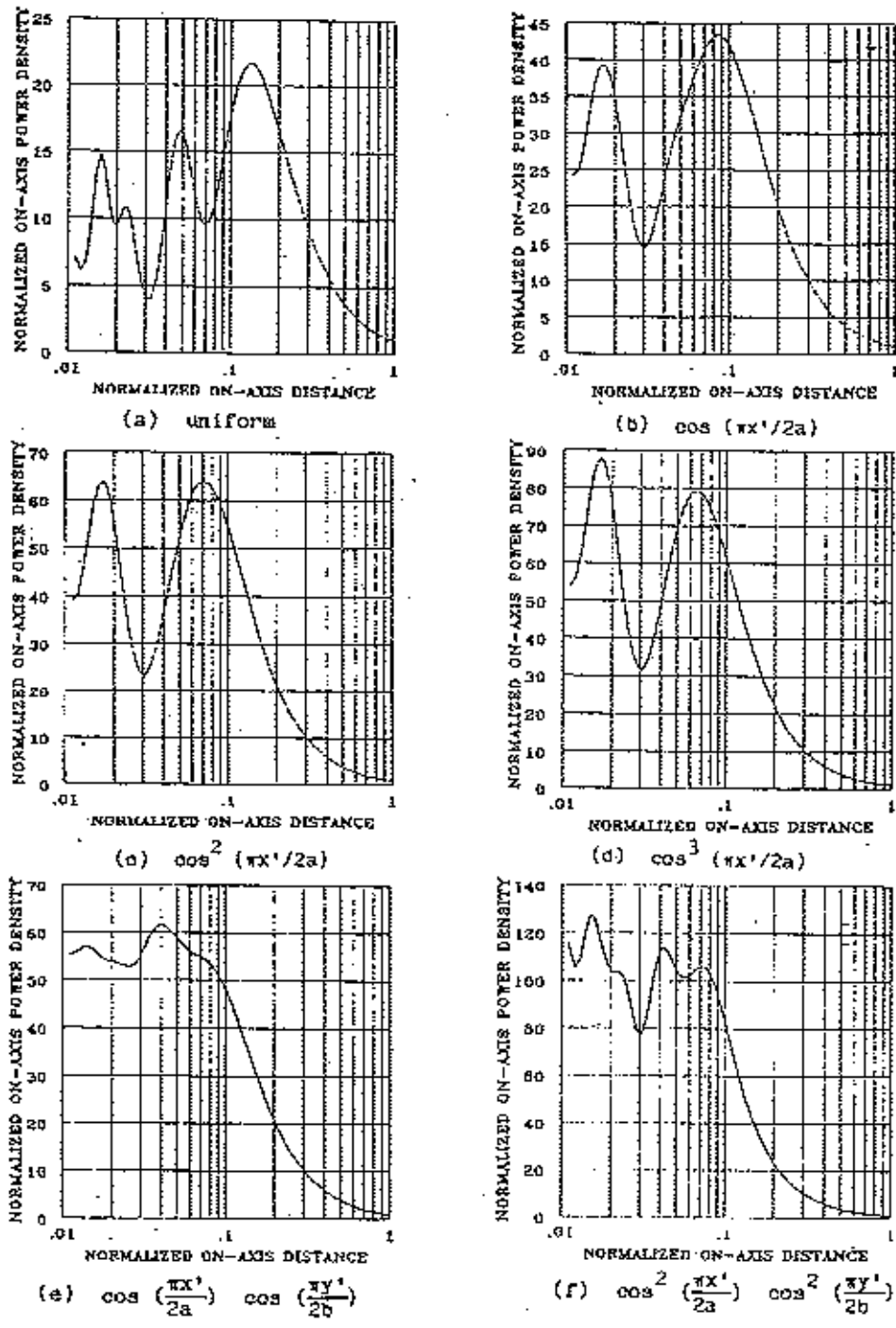
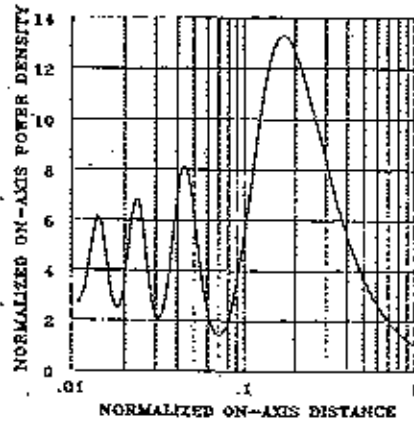
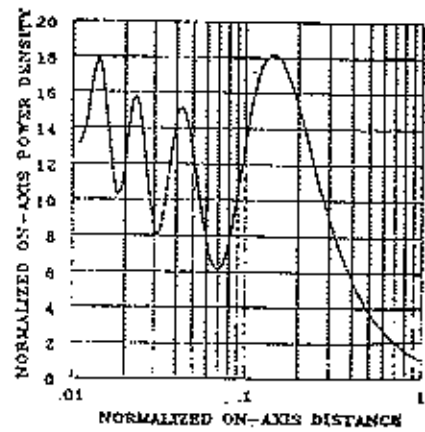


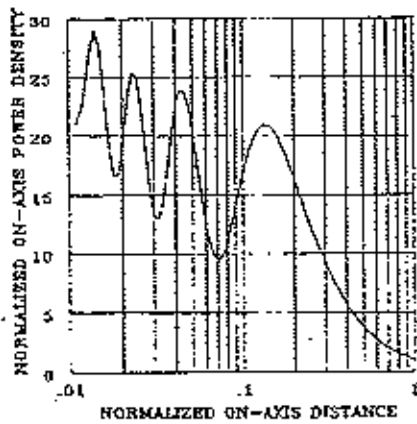
Figure 4-15. Correction factor vs. on-axis distance normalized to  $8a^2/\lambda$  for rectangular aperture with dimensions  $a/\lambda=15$ ,  $b/\lambda=10$ , and different distribution functions.



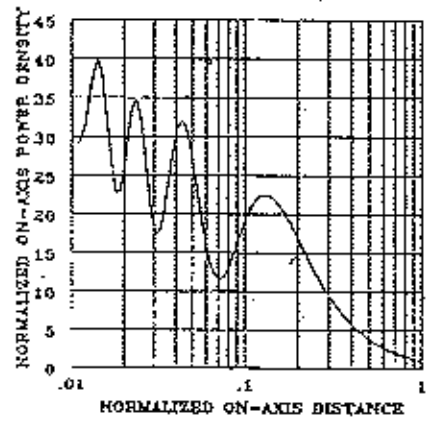
(a) uniform



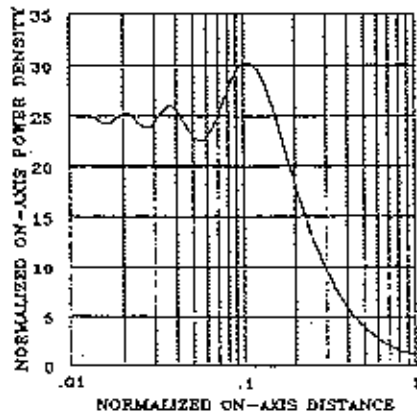
(b)  $\cos(\pi x'/2a)$



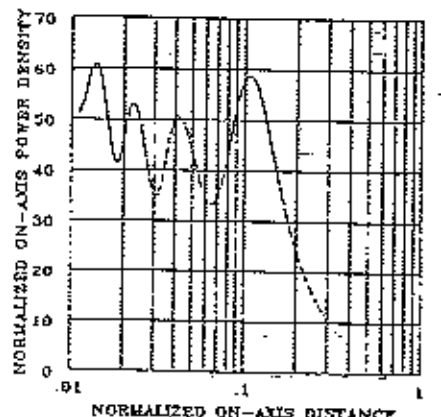
(c)  $\cos^2(\pi x'/2a)$



(d)  $\cos^3(\pi x'/2a)$



(e)  $\cos\left(\frac{\pi x'}{2a}\right) \cos\left(\frac{\pi y'}{2b}\right)$



(f)  $\cos^2\left(\frac{\pi x'}{2a}\right) \cos^2\left(\frac{\pi y'}{2b}\right)$

Figure 4-16. Correction factor vs. on-axis distance normalized to  $8a^2/\lambda$  for rectangular aperture with dimensions  $a/\lambda=15$ ,  $b/\lambda=15$ , and different distribution functions.

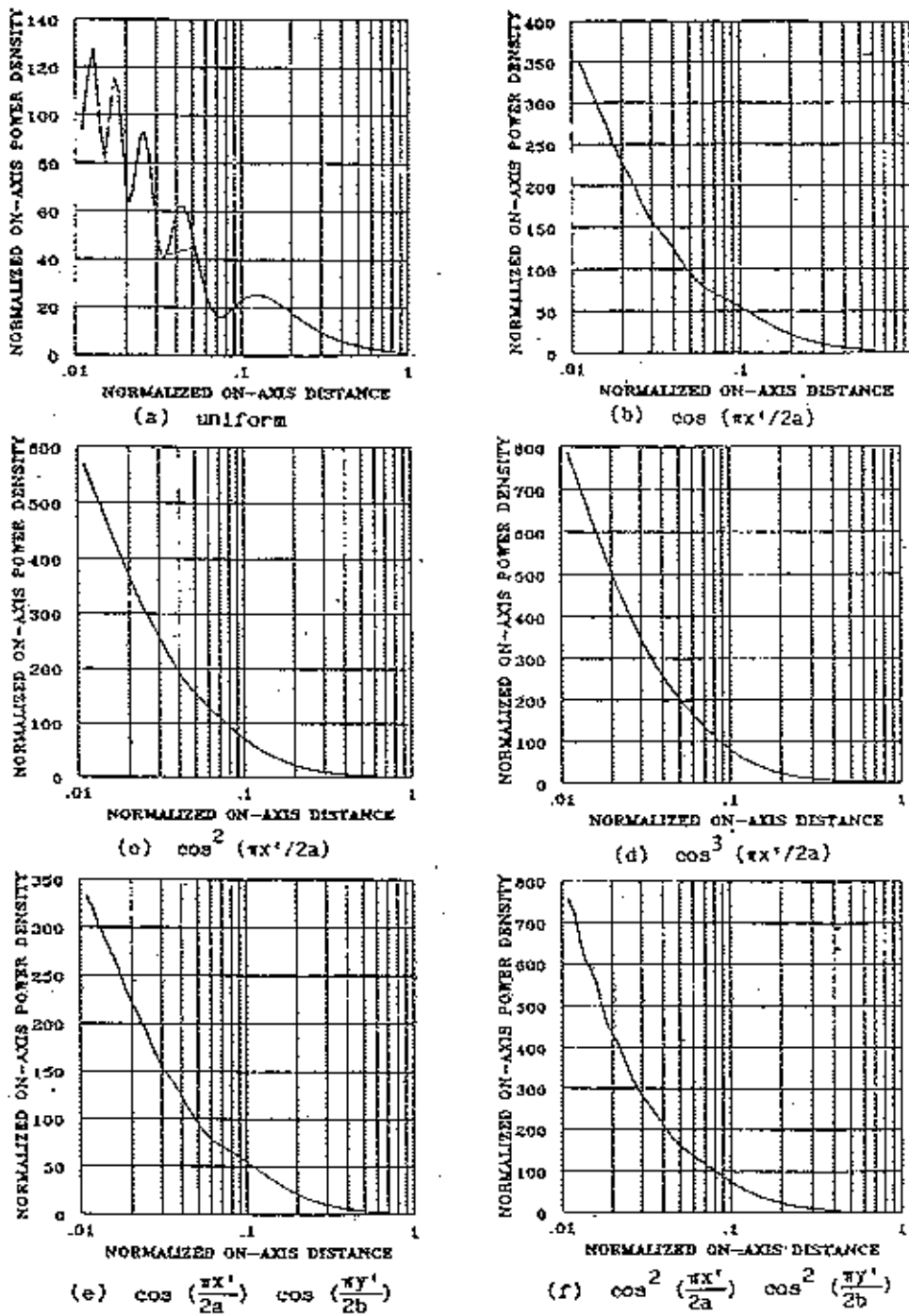
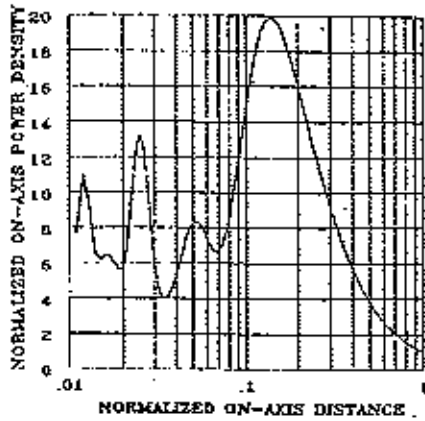
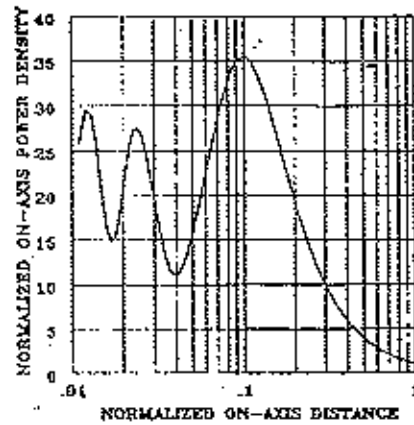


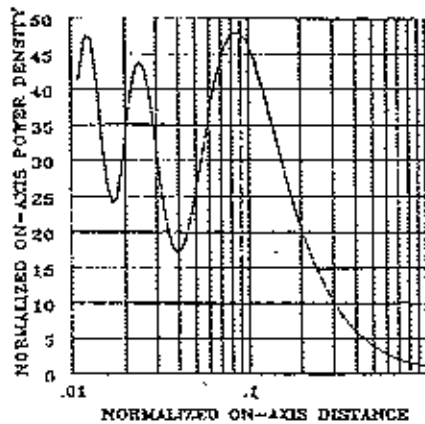
Figure 4-17. Correction factor vs. on-axis distance normalized to  $8a^2/\lambda$  for rectangular aperture with dimensions  $a/\lambda=20$ ,  $b/\lambda=5$ , and different distribution functions.



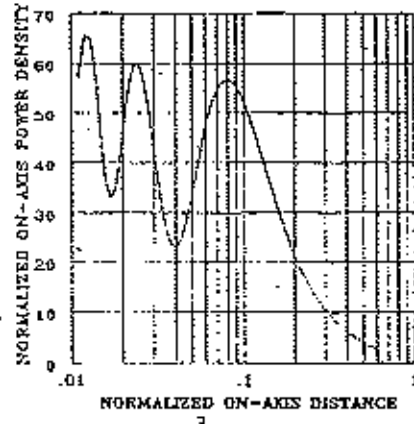
(a) Uniform



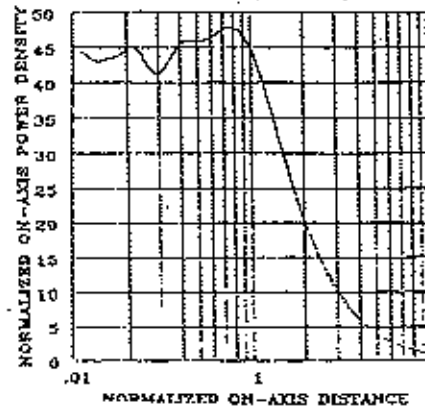
(b)  $\cos(\pi x'/2a)$



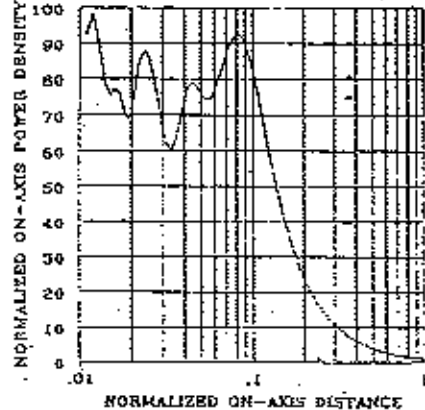
(c)  $\cos^2(\pi x'/2a)$



(d)  $\cos^3(\pi x'/2a)$



(e)  $\cos\left(\frac{\pi x'}{2a}\right) \cos\left(\frac{\pi y'}{2b}\right)$



(f)  $\cos^2\left(\frac{\pi x'}{2a}\right) \cos^2\left(\frac{\pi y'}{2b}\right)$

Figure 4-18. Correction factor vs. on-axis distance normalized to  $8a^2/\lambda$  for rectangular aperture with dimensions  $a/\lambda=20$ ,  $b/\lambda=15$ , and different distribution functions.

Substituting Equations (4-7) and (4-8) into (4-9) and carrying out the integration we obtain the far field pattern for each distribution function. This integration is rather straightforward. The characteristics for the far field pattern produced by a rectangular aperture for different distribution functions were obtained. The results of such calculations are summarized in Tables 4-3 and 4-4.

TABLE 4-3

FAR FIELD CHARACTERISTICS OF RECTANGULAR APERTURES WITH  
 $\cos^n \frac{\pi x'}{2a}$  DISTRIBUTION FUNCTIONS

n	Full Width At Half Power (Radian)		First Sidelobe dB Below Peak Intensity	
	Horizontal Plane	Vertical Plane	Horizontal Plane	Vertical Plane
0	$0.88 \frac{\lambda}{2a}$	$0.88 \frac{\lambda}{2b}$	13.2	13.2
1	$1.20 \frac{\lambda}{2a}$	$0.88 \frac{\lambda}{2b}$	23	13.2
2	$1.45 \frac{\lambda}{2a}$	$0.88 \frac{\lambda}{2b}$	32	13.2
3	$1.66 \frac{\lambda}{2a}$	$0.88 \frac{\lambda}{2b}$	40	13.2



TABLE 4-4

FAR FIELD CHARACTERISTICS OF RECTANGULAR APERTURES WITH  
 $\cos^n \frac{\pi x'}{2a}$     $\cos^n \frac{\pi y'}{2b}$    DISTRIBUTION FUNCTIONS

n	Full Width At Half Power (Radian)		First Sidelobe dB Below Peak Intensity	
	Horizontal Plane	Vertical Plane	Horizontal Plane	Vertical Plane
1	$1.20 \frac{\lambda}{2a}$	$1.20 \frac{\lambda}{2b}$	23	23
2	$1.45 \frac{\lambda}{2a}$	$1.45 \frac{\lambda}{2b}$	32	32

The data in Tables 4-3 and 4-4 show the correspondence between the parameter  $n$  and the far field parameters such as sidelobe levels. Using, for example, the sidelobe level for the antenna given in the NTIA Form 35 for a system, one can readily determine  $n$  for that antenna using the data in Tables 4-3 and 4-4 as appropriate. Once  $n$  is determined, the near field correction factor for the antenna may be obtained with the aid of the data given in Figures (4-6) to (4-18). This procedure is further clarified through examples later in this section.

The off-axis analysis for rectangular aperture was not attempted during this analysis. Such results are not available in the literature at this time in a form appropriate to the objective of this task. However, the results for off-axis calculation may be incorporated in the follow-up effect at a later date.

Applications of Analysis Procedure

Two examples, one associated with circular apertures and the other with rectangular apertures are discussed here to illustrate the calculation procedure formulated in this section. The circular aperture will be treated first.

Given the following data for a circular dish antenna, determine the maximum on-axis power density:

First sidelobe level (dB).....	30.6
Frequency (GHz).....	3.0
Transmitter power (Watts).....	1.0
Antenna gain (dBi).....	38.0
Beamwidth (degrees).....	2.25

Determine the parameter  $n$  and beamwidth (BW) from the data in Table 4-1 for the aperture with 30.6 dB sidelobe level. In Table 4-1, the values of  $n$  and BW for the antenna with 30.6 dB sidelobe are 2 and  $1.46 \lambda/D$ , respectively. Using this information:

$$\begin{aligned} BW &= 1.46 \lambda/D \\ 2.25 \times \pi/180 &= 1.46 \lambda/D \\ D/\lambda &= 37.7 \end{aligned}$$

Next, we calculate the far field power density at  $2D^2/\lambda$  along the antenna axis.

$$P_d = \frac{P_t G_t}{4\pi\lambda^2 (2D^2/\lambda)^2}$$

or

$$P_d = \frac{10^{3.8} \times 1000}{1600 \pi \times (37.7)^4} = .00062 \text{ mW/cm}^2$$

The maximum on-axis power density may now be evaluated by multiplying  $P_d$  given above by correction factor given in Figure 4-3(d). Therefore, the maximum power density at a distance  $0.14 D^2/\lambda$  will be

$$\text{maximum power density} = 70 \times .00065 = .0435 \text{ mW/cm}^2$$

which is the desired result.

Note that the power density at any other point along the axis may be evaluated in a similar manner by using the data in Figure 4-3(d).

The calculation of on-axis power density for a rectangular aperture is similar to that described above for the circular dish. For rectangular apertures, we use the data in Table 4-3 or 4-4 for determination of  $n$  and data in Figures 4-6 to 4-18 for the appropriate correction factor. To illustrate this procedure further, let us assume that the following data is known for a rectangular aperture.

First sidelobe level (horizontal plane).....	23
First sidelobe level (vertical plane).....	13.2
Frequency (GHz).....	3
Transmitter power (Watts).....	1
Antenna gain (dBi).....	35
Beamwidth (horizontal plane), deg.....	1.7
Beamwidth (vertical plane), deg.....	2.52

(Note that NTIA Form-35 does not specifically include information on sidelobe levels for both vertical and horizontal planes associated with rectangular apertures on non-symmetrical distributions. However, the form has information on vertical and horizontal beamwidths. When the data on sidelobe

levels is not available, the data on beamwidths given in Form-35 may be used to determine the appropriate distribution with the aid of information in Tables 4-3 or 4-4). Using the data for the sidelobe levels and/or beamwidths given above, the distribution function for this example may be determined with the aid of the data given in Table 4-3. Hence, the distribution function is uniform in the vertical plane and cosinusoidal in the horizontal plane. From Table 4-3, we have

$$\begin{aligned} \text{Beamwidth (horizontal plane)} &= 1.2 \frac{\lambda}{2a} = 1.7 \times \frac{\pi}{180} = .03 \\ a/\lambda &= 20.2 \end{aligned}$$

also

$$\begin{aligned} \text{Beamwidth (vertical plane)} &= .88 \frac{\lambda}{2b} = 2.52 \times \frac{\pi}{180} = .04 \\ b/\lambda &= 10 \end{aligned}$$

The correction factor for this aperture may be obtained from the curve in Figure 4-6(b). The maximum correction factor is 75. By definition, the correction factor for this example is

$$\text{correction factor} = \frac{\text{on-axis power density in the near field}}{\text{on-axis power density at } 8a^2/\lambda} = 75$$

The on-axis power density at  $8a^2/\lambda$  may be obtained from the formula

$$P_d = \frac{P_t G_t}{4\pi\lambda^2 \left(8 \frac{a^2}{\lambda}\right)^2} \quad (4-8)$$

Using the given data noted above we have

$$P_d = \frac{1000 \times 10^{3.5}}{256\pi \times 100 \times (20.2)^4} = 2.45 \times 10^{-4} \text{ mW/cm}^2 \quad (4-9)$$

Hence, the maximum power density in the near field may be obtained by multiplying  $P_d$  by the maximum correction factor. Therefore

$$\text{maximum power density} = 2.45 \times 10^{-4} \times 75 = 0.018 \text{ mW/cm}^2$$

which is the desired result.

It is important to point out that in practice, the data for an antenna may not match the data given in Table 4-3 or 4-4. For estimating the power density in the near field, only an approximate match between the data for the antenna under the consideration and the data in these tables is sufficient to provide the necessary assessment at this time.

#### Linear Antenna

Techniques for the computation of near field in thin wire antennas have been reported in the past [Adams, A. T.; Baldwin, T. E.; and Warren, E., 1978]. The techniques include moment methods which have been used to treat a wide variety of radiation and scattering problems in electromagnetic. A number of algorithms including Numerical Electromagnetic Code (NEC) have been developed in the last decade using the moment methods.

The NEC computer model was used to develop simplified models for the near field calculation of wire antennas by the NTIA. A description of this model was given earlier in this section. The model was found useful to treat the majority (75%) of wire antennas listed in the GMF. These antennas are listed under the following names in the GMF:

1. Dipole
2. Monopole
3. Whip
4. Log Periodic

5. Yagi
6. Collinear

Wire antennas used in the government telecommunication system and not included in the above will be treated later in a follow-on effort.

#### Some Thoughts on Near Field Calculations of Wire Antennas

For convenience and generality, it is appropriate to accept as a thesis that a half-wave dipole is an analytical building block for all the wire antennas listed above. In fact, physically, the last three linear antenna types listed in the previous subsection are a collection of dipole antennas placed in a specific arrangement. This concept results in a simplified model which may be used to calculate the field intensity for any one of these antennas by using an appropriate correction factor as a multiplier for the field of an electric dipole. More detailed discussion of this multiplier for each specific antenna will be given later.

Radiation hazard assessments of wire antennas may not need near field calculation. For example, a half-wave dipole antenna at 300 MHz with a 100 kw transmitter is capable of producing a maximum of 1478.8 volts/m field intensity at  $1.5\lambda$  meters away. This field intensity exceeds 194.2 volts/m level which corresponds to  $10 \text{ mw/cm}^2$ . Note that for this assessment near field analysis was not necessary, since if the system exceeds this limit in the far field it will exceed the criteria in the near field as well.

Another point which must be mentioned here pertains to wire antennas used at very low frequencies (below 30 MHz). Not every dipole antenna in the GMF is necessarily a half wavelength long. A halfwave dipole at 1 MHz is 150 meters long. Practical considerations prohibits the use of such antennas for mobile service systems. A wire antenna used in mobile service at low frequencies may be a fraction of a wavelength long. If a wire antenna is approximately equal or less than a tenth of a wavelength long, it should be treated as a current element. Closed form expressions for both the free space

near and far field intensities of a current element may be found in text books on electromagnetic theory, see for example [Kraus, J. D., 1950] or [Harrington, R., 1968]. For systems in which such electrically short antennas are placed over the ground plane with 100% ground reflection, a good approximation may be achieved by multiplying the free space calculation results by a factor of 2 [Cleveland, R.F. 1985].

Simplified wire antenna models given in this section should be used in the radiation hazard assessment only after the above considerations were found to be inapplicable.

Dipole Antenna. Dipole antennas are used in a large number of telecommunication systems registered in the GMF. The simplicity, relatively low cost, and desirable electrical characteristics are among the many reasons which contribute to the popularity of dipole antennas.

At very low frequencies dipole antennas are electrically small and as such may be treated as a short electric dipole. From the analysis point of view this is very fortuitous, since closed form solutions exist for a short electric dipole that describe the near field or far field relationships. To facilitate the radiation hazard assessment of such antennas, the expressions describing the radiation from these antennas are given below [Harrington, R., 1961]. Figure 4-19 shows the orientation of a short dipole in free space. The equations describing the fields of a short dipole (current element) are,

$$E_r = \frac{I l}{2\pi} e^{-jkr} \left( \frac{\eta}{r^2} + \frac{\eta}{jkr^3} \right) \cos\theta \quad (4-10)$$

$$E_\theta = \frac{I l}{4\pi} e^{-jkr} \left( \frac{jk\eta}{r} + \frac{\eta}{r^2} + \frac{\eta}{jkr^3} \right) \sin\theta \quad (4-11)$$

$$H_\phi = \frac{I l}{4\pi} e^{-jkr} \left( \frac{jk}{r} + \frac{1}{r^2} \right) \sin\theta \quad (4-12)$$

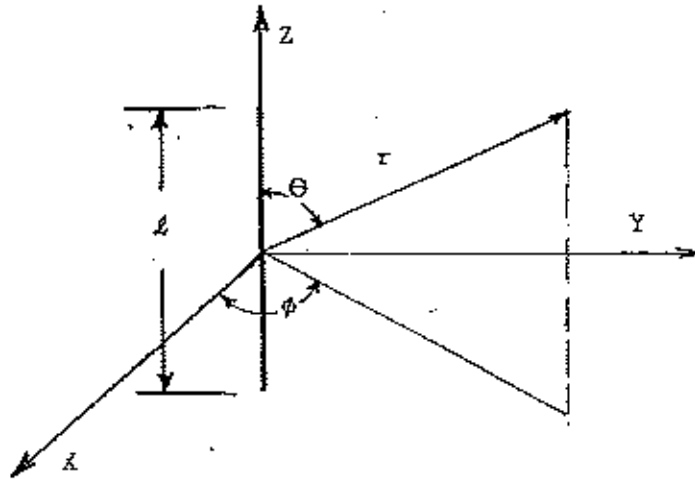


Figure 4-19. Geometry of a short electric dipole (current element).

where  $k$  is the propagation constant and  $\eta$  is the intrinsic impedance of the free space. Very close to the current element, the  $E$  field reduces to that of a static charge dipole, the  $H$  field reduces to that for a constant current element and the field is said to be quasi-static. The relationships (4-10), (4-11), and (4-12) are applicable to both far and near fields when the short electric dipole is in free space.

In practice nearly all such antennas are either over an infinite or finite ground plane. Treatment of an electric current element over the ground is more difficult and may not be necessary for the analysis given here. A good approximation may be obtained by multiplying the expressions in 4-10 to 4-12 by a factor of 2 to include the ground reflection.



In the derivation of Equations 4-10 to 4-12 the assumption was that the current along the element is constant. As the length of the element grows larger this assumption is no more valid. In the case of a center-fed linear antenna, a very good approximation is to assume that the current distribution on the antenna is sinusoidal [Kraus, 1950]. Current-distribution measurement indicate that this is a good approximation provided that the antenna cross section is small compared to a wavelength. This assumption excludes some of the so-called fat dipole antennas which are sometimes used at microwave frequencies. Jordan [1968] has derived closed form expressions for the fields produced by a dipole assuming sinusoidal current distribution. These expressions given below are valid for both far field and near field.

$$E_r = -j30I_m \left( \frac{e^{-j\beta R_1}}{R_1} + \frac{e^{-j\beta R_2}}{R_2} - 2 \cos \beta H \frac{e^{-j\beta r}}{r} \right) \quad (4-13)$$

$$E_\theta = j30I_m \left( \frac{z-H}{y} \cdot \frac{e^{-j\beta R_1}}{R_1} + \frac{z+H}{y} \cdot \frac{e^{-j\beta R_2}}{R_2} - \frac{2z \cos \beta H}{y} \frac{e^{-j\beta r}}{r} \right) \quad (4-14)$$

$$H_\phi = \frac{j30I_m}{\eta y} (e^{-j\beta R_1} + e^{-j\beta R_2} - 2 \cos \beta H e^{-j\beta r}) \quad (4-15)$$

Where  $I_m$  is the maximum amplitude of current along the length of the antenna. Figure 4-20 shows some of the notations used in the expressions (4-13) to (4-15).

A computer algorithm using Equations 4-13 to 4-15 was prepared for calculating the electric field along the Y axis. The results of such calculations are shown in Figure 4-21.

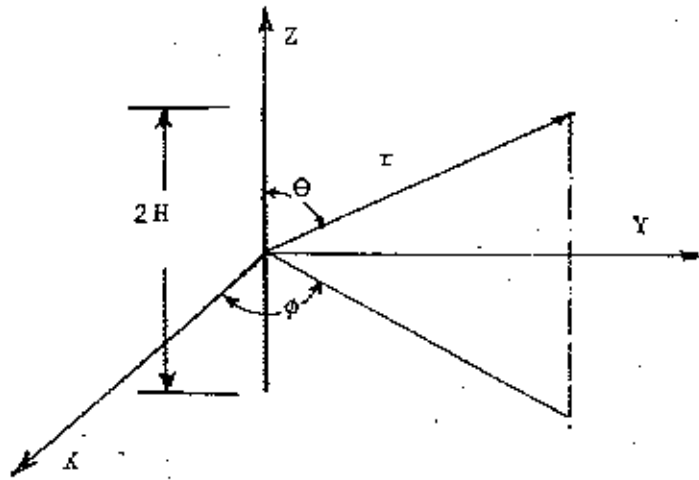


Figure 4-20. Geometry for a dipole antenna.

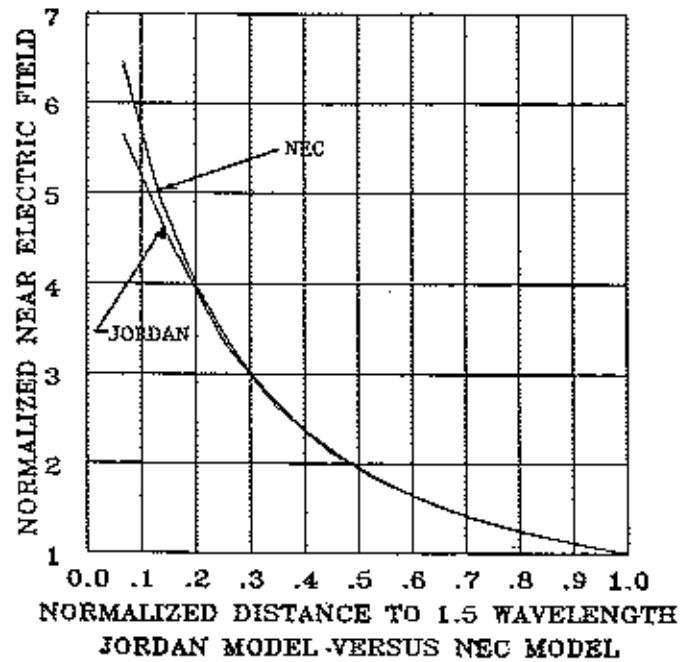
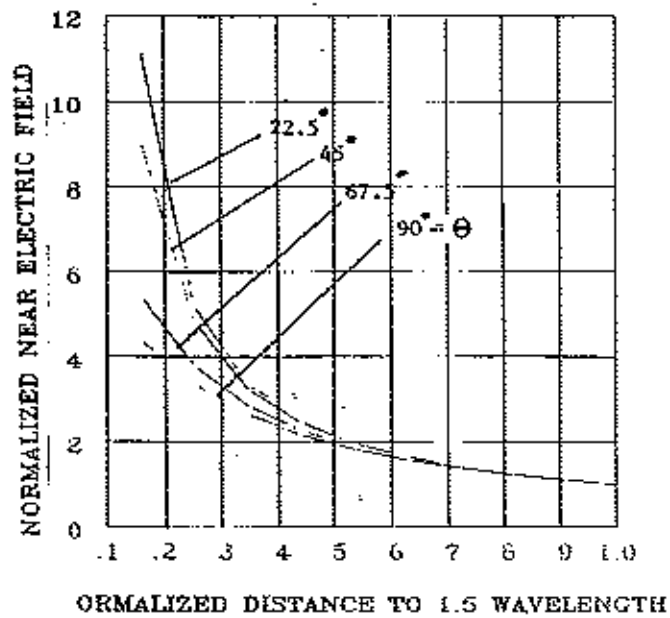


Figure 4-21. A plot of the normalized electric field along the y-axis.

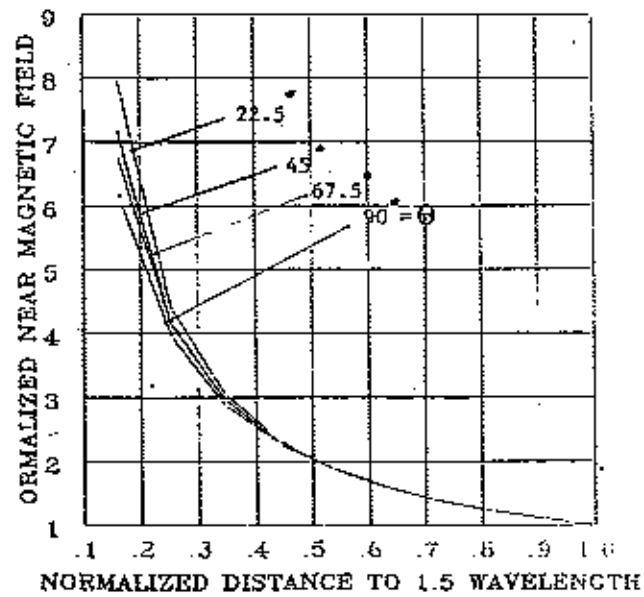
The curve designated Jordan in Figure 4-21 shows the calculated field along the Y axis using a computer program based on Equations 4-13 to 4-15. Note that these equations describe the fields of a dipole at all points surrounding the antenna.

The accuracy of the results obtained using Equations 4-13 to 4-15 was determined through comparison with the calculations obtained using NEC model, described earlier in this report. The results obtained using NEC for the same antenna was also plotted in Figure 4-21. Note that results obtained using Jordan's derivations are in good agreement with those obtained from the NEC model. Hence, Equation 4-13 to 4-15 provide a convenient method for assessing the field intensities produced by a dipole in free space. In practice, however, nearly all such antennas are located over an electrically infinite or finite ground plane. To facilitate the calculation of the fields for these antennas, the results obtained using Equations 4-13 to 4-15 may be multiplied by a factor of two to include the reflection from the ground plane.

The results shown in Figure 4-21 are applicable only to on-axis calculations. However, there are occasions where off-axis assessment may be necessary. Data in Figure 4-22 includes the correction factor for off-axis points on a sphere surrounding the half-wave dipole in the free space. Calculation of the field intensities are made for  $\theta=22.5^\circ$ ,  $45^\circ$ ,  $67.5^\circ$ , and  $90^\circ$ . Similar data for a full-wave dipole are shown in Figure 4-23. Note that data for H-field is also included in Figures 4-22 and 4-23. The data on the horizontal axis was normalized to  $1.5 \lambda$  and the data on the vertical axis was normalized to the field at a location  $1.5 \lambda$  away from the dipole. The data shown in Figures 4-21 through 4-23 are essential to the analysis of linear antennas discussed here and we will have occasion to use the information in these figures to assess the radiation hazards of other linear antennas such as a log periodic, Yagi, or collinear dipole antennas. A brief description of each antenna type together with the procedure used in assessing their near field intensities are given here.

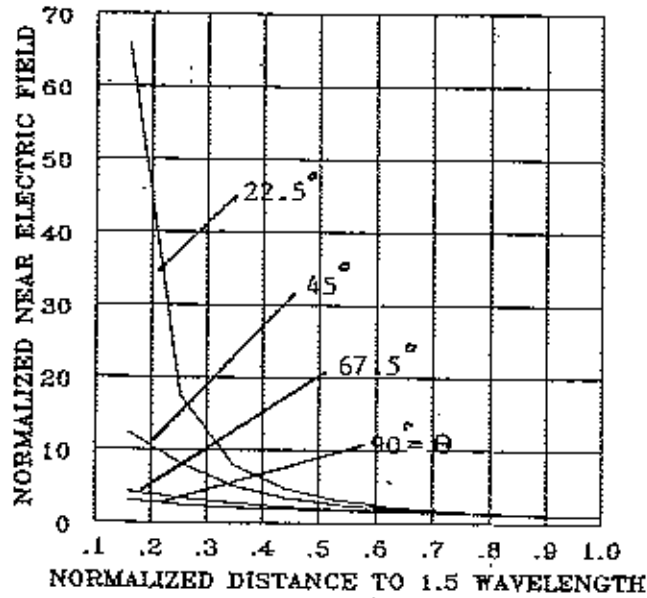


(a)

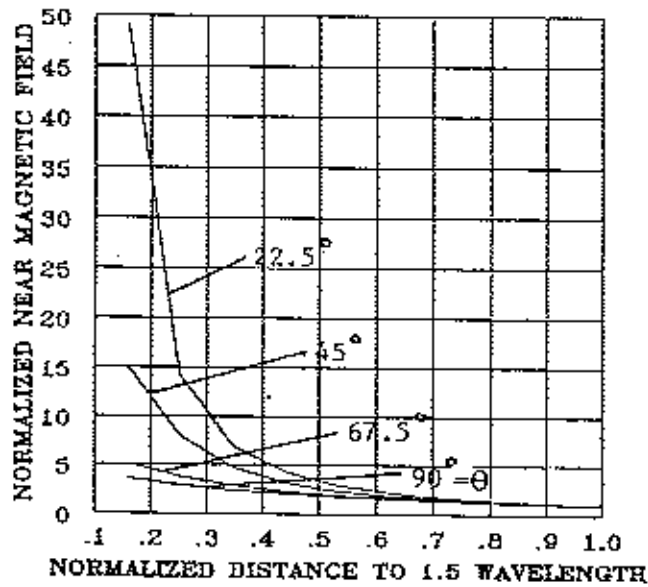


(b)

Figure 4-22. Correction factor vs. distance normalized to  $1.5\lambda$  away from a half-wave dipole in free space, (a) electric field, (b) magnetic field.  $\theta$  is the polar angle shown in Figure 4-20.



(a)



(b)

Figure 4-23. Correction factor vs distance normalized to  $1.5 \lambda$  away from a full-wave dipole in free space, (a) electric field, (b) magnetic field.  $\theta$  is the polar angle shown in Figure 4-20.

Monopole. A monopole antenna consists of a straight wire perpendicular to a ground plane, as shown in Figure 4-24.

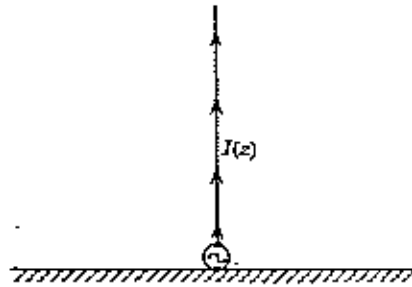


Figure 4-24. The monopole antenna geometry.

Using the imaging technique it is easy to show that the field of a monopole antenna is the same as that from a dipole antenna Figure 4-20 fed at the center.

Whip. Whip antennas constitute a large category of vehicular antennas. A whip antenna is different from that of a monopole because the feed point for a whip is not necessarily at the ground plane. A large variety of whip antennas are commercially available and are used in the government telecommunication systems. Several examples as shown in Figure 4-25.

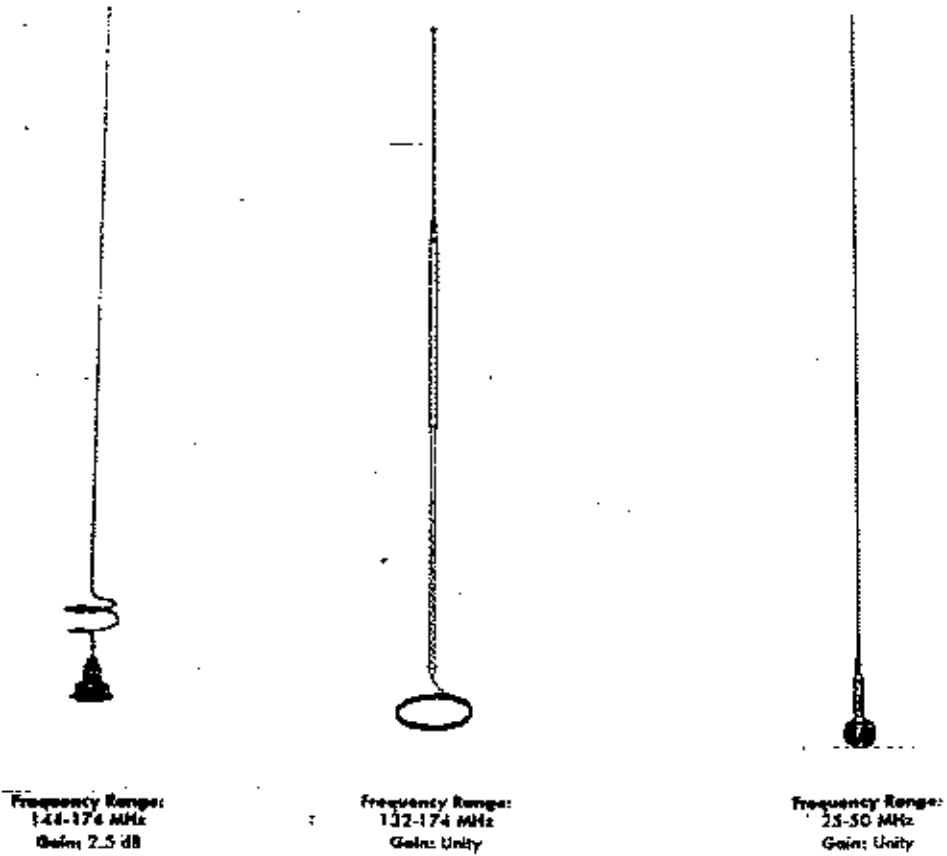


Figure 4-25. Three different types of whip antennas designed for use on vehicles.

Whip antennas have generally low gain and their far field characteristics are similar to those of a dipole. The NEC model was used to find a comparison between the near field intensity of a dipole and a typical whip antenna. The results indicated that the near field of a whip may be approximated by that obtained from a dipole. Whip antennas are used with both high power (Kw) and lower power (1 watt) transmitters. In land mobile applications the transmitters generally range from 1 watt to 110 watts.

Log Periodic. A log periodic antenna generally consists of a number of dipoles of different length. Gain values as high as 16 dB are achievable with log periodic antennas. They are used in the frequency range 4 to 32 MHz and at VHF frequencies below 1 GHz. Output power of the transmitter connected to a log periodic may vary from several watts to as high as 50 KWatts. The physical size of log periodic antennas at HF frequency is quite large and a projection of the antenna on the ground including the necessary guywires may cover a rectangle of 80 m x 60 m, see Figure 4-26.

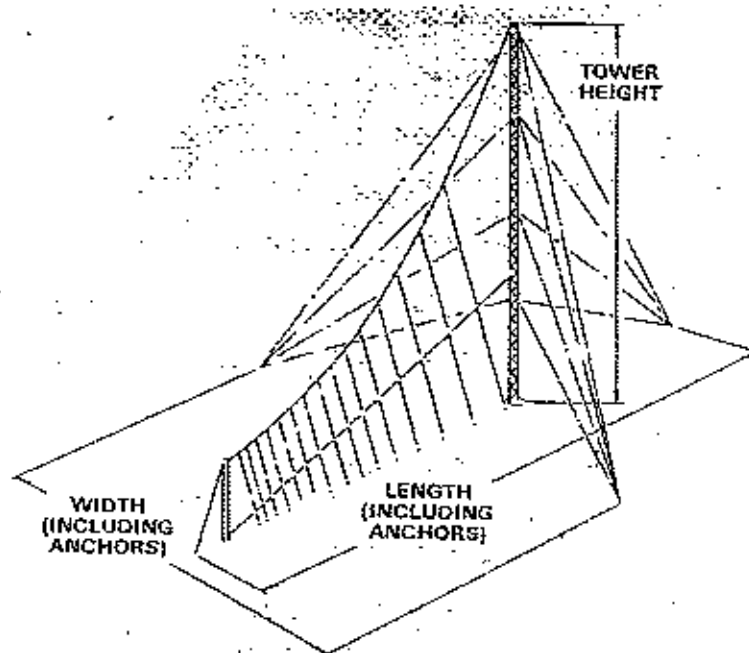


Figure 4-26. Structures of a H.F. log periodic antenna.

VHF log periodic antennas are mounted on a mast approximately 14 m above the ground, see Figure 4-27. The antenna elements can be vertical or horizontal depending on the desired polarization.



Log periodic antennas constitute an important class of antennas used in telecommunications. Because of the relatively high gain and high transmitter power used with these antennas, their radiation hazard assessments require care. The desired model intended for the analysis of log periodic antennas needs to be simple and yet conservative.

Since a log periodic consists of an array of dipoles of different length, it is feasible to assume that as a first-order approximation, the field produced by a log periodic is the sum total of the fields produced by each of the dipoles in the array. This assumption ignores the coupling effects that exist between the elements of the array. However, the effect of the coupling is generally not serious since the dipoles in the array vary in length and at any given frequency only a few of the dipoles operate in resonance.

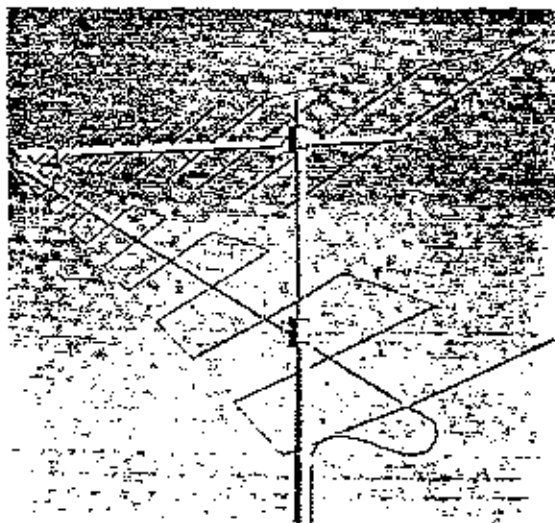
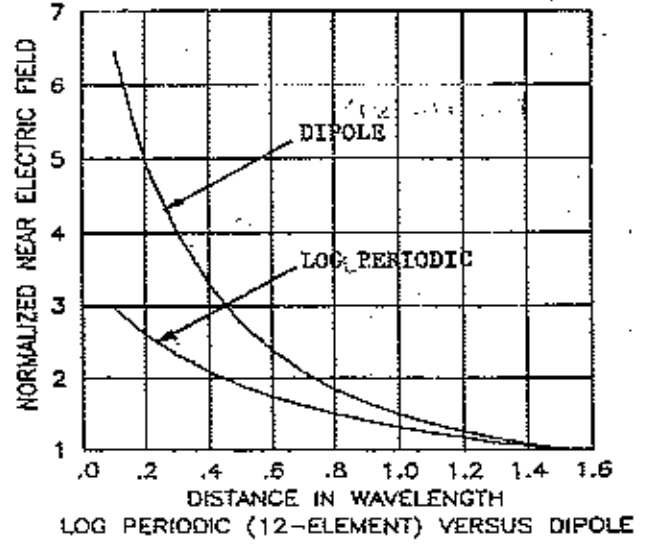
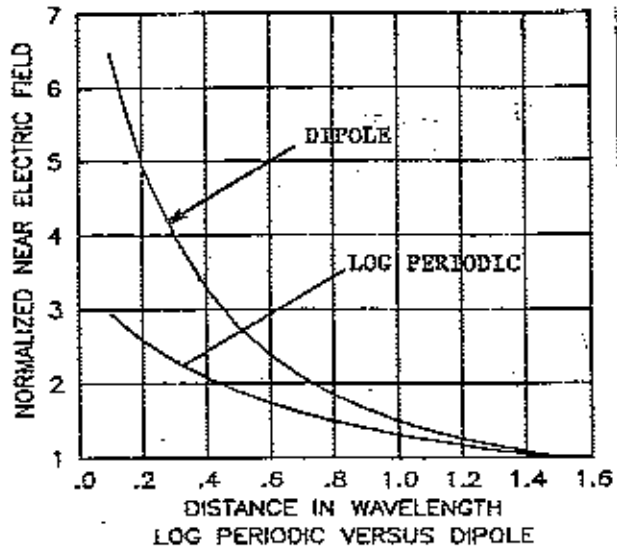
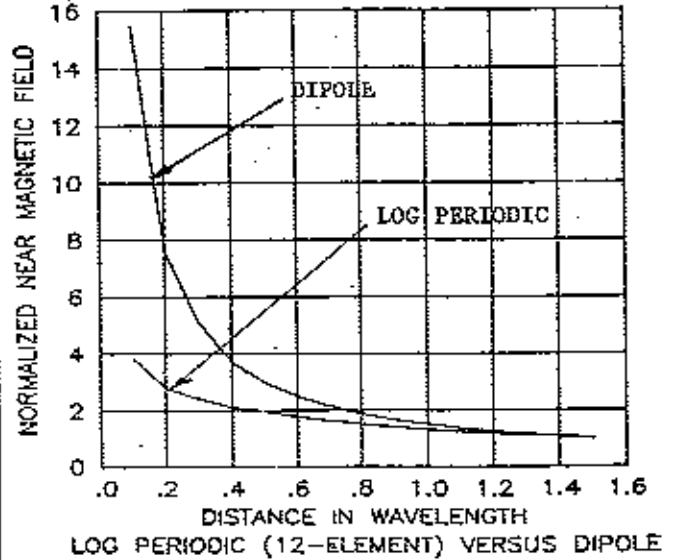
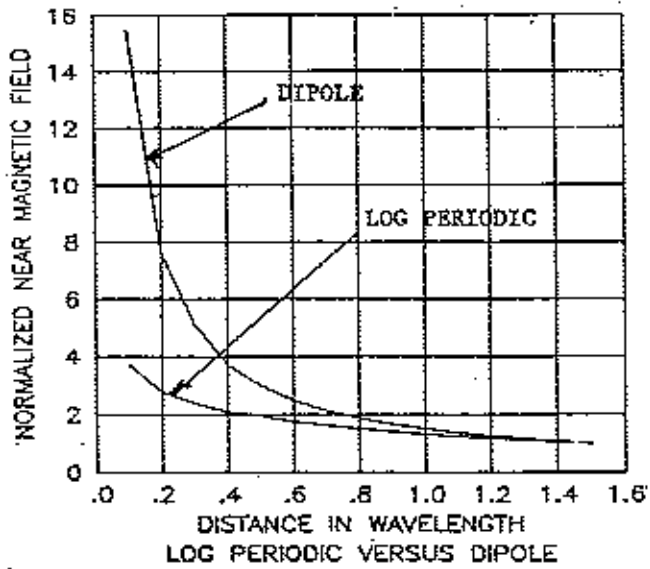


Figure 4-27. Log-periodic wire trapezoid antenna.

The NEC model was used to calculate the maximum near field intensity produced by an eight-element log periodic antenna. The results obtained by a computer model are plotted in Figure 4-28. Note that the results obtained by the model include the effect of the mutual coupling between the dipole elements in the log periodic. Figure 4-28(a) shows the comparison for the electric field whereas Figure 4-28 (b) shows a comparison of the magnetic field. The distance in wavelength shown in this figure was measured along the



(a) Electric Field



(b) Magnetic Field

Figure 4-28. Comparison of normalized field intensity of electric dipole with that produced by an eight or 12 element log periodic antenna.

direction of maximum propagation. The data shown in these figures are for antennas operating at 40 MHz. Note that in both cases the correction factor plotted on the vertical axis for the single dipole has a higher value than the corresponding one for the log periodic antenna. Hence, the correction factor for a dipole constitutes a conservative multiplying factor for a log periodic antenna. The calculation procedure for assessing the electric or magnetic fields of a log periodic is discussed later in this section.

Yagi Antenna. Directional arrays can be constructed in which currents are induced in the non-driven elements by the fields of a driven element. This arrangement is the basic concept used in the design of a class of antenna whose performance was demonstrated by H. Yagi in 1928. The non-driven elements shown in Figure 4-29 have no transmission-line connection with the transmitter and are usually referred to as parasitic elements. Some of the parasitic elements are called directors and are located in front of the driven element while the remaining parasitic element is called reflector and is usually located behind the driven element as shown in 4-29. Note that elements in a Yagi antenna are nearly equal in length while the spacing between them vary. The reason for different spacing between the elements is to adjust the phase of the induced current in the parasitic elements. The proper phasing for the induced current provides the desired directivity for the antenna.

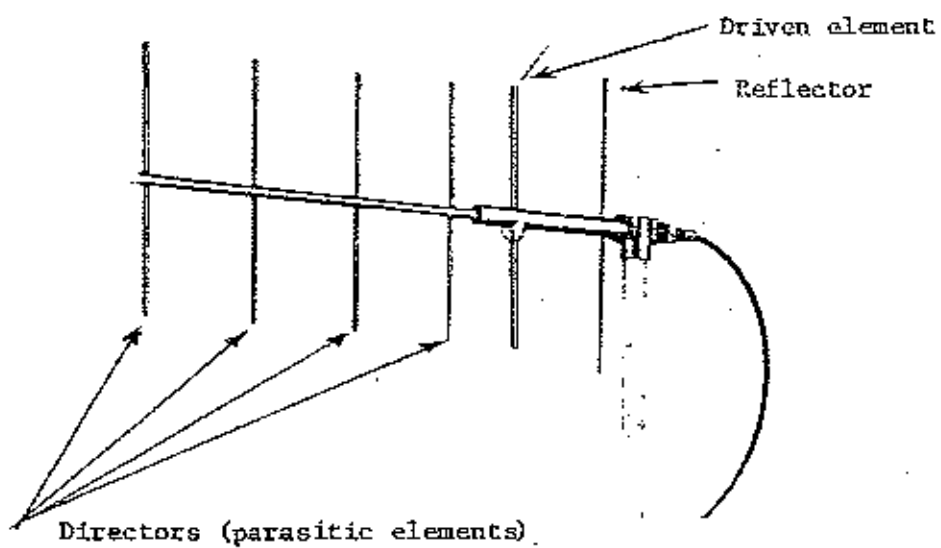
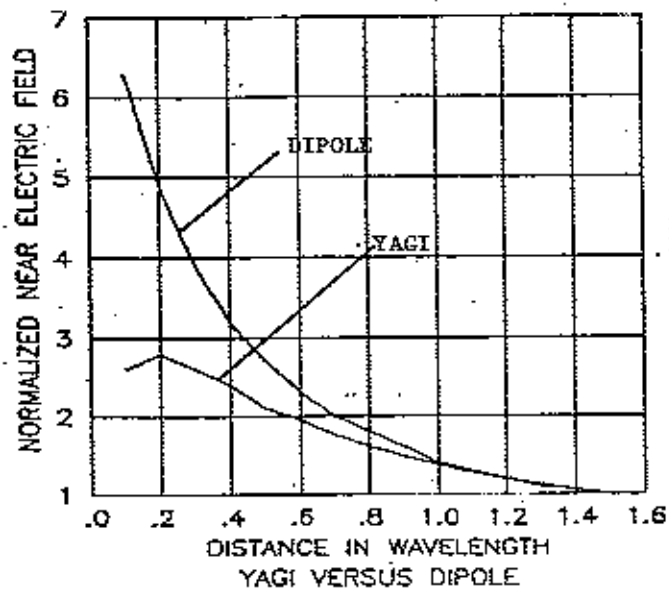


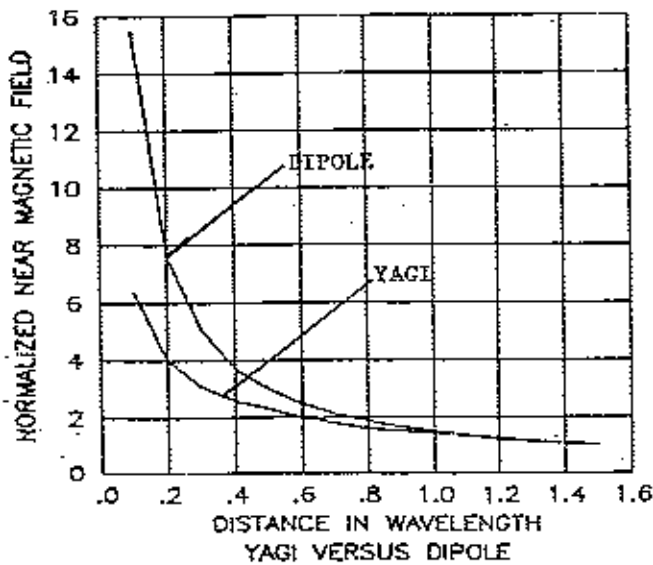
Figure 4-29. A six-element Yagi antenna.

Several thousand assignments in the GMF indicate that Yagi antennas are used in many the Government telecommunication systems designed to operate in the VHF region. Yagi antennas are capable of producing gains as high as 12 dBi and is generally rated to operate with transmitters having output up to 600 watts of RF power.

The NEC model was used to calculate the normalized field intensity at points along the axis of the Yagi antenna. The results of the calculation are shown in Figure 4-30. The normalized field intensity produced by a dipole with input power equal to that for the Yagi antenna was also obtained using the NEC computer model. Figure 4-30 shows a plot of the normalized field intensity for the dipole. The data shown in Figure 4-30 were obtained using identical input power with no loss for both Yagi and dipole. Both antennas were matched to 50 ohm transmission line. Note that the value of correction factors for the dipole remain above those for the Yagi at all points along the on-axis distance. Hence using the correction factor for the dipole in the calculation of the near field intensities for Yagi antenna will yield results which would be conservative. This level of conservatism was assumed necessary in the simplified procedure presented here.



(a) Electric Field



(b) Magnetic Field

Figure 4-30. Comparison of correction factor for a single dipole with that of a Yagi antenna.

Collinear Antennas. High gain collinear antennas are often used at the base stations. Collinear with lower gain, generally consisting of two or three elements, have been used on vehicles. These vehicular antennas are sometimes installed on the roof or the trunk of vehicles. Base station antennas have gains as high as 12 dB as compared to the lower gain version which have approximately 3 dB gain. An additional important feature of these antennas is the omnidirectional pattern with main beam pointed at low elevation angle. This is accomplished by using half-wave dipoles in tandem and all fed in phase. Figure 4-31 illustrates this design concept used in a two-element collinear antenna.

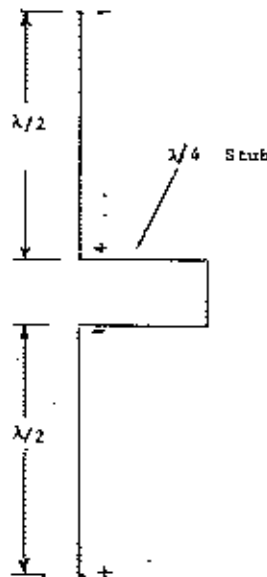
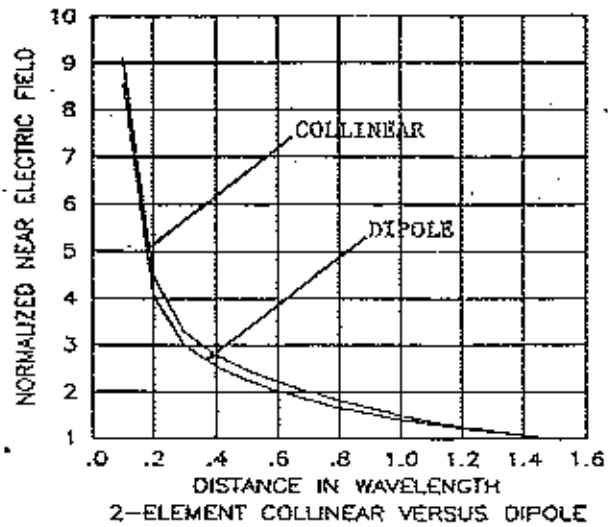


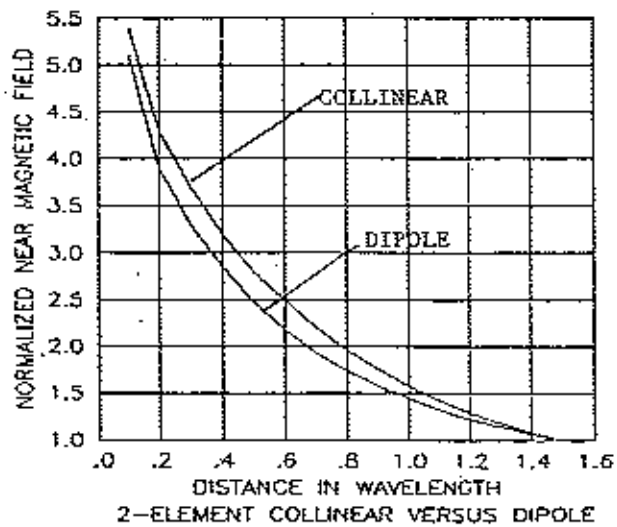
Figure 4-31. Design of a collinear antenna.

The phase correction is performed by means of a quarter-wave stub placed between two consecutive half-wave dipoles.

There are approximately 24000 assignments in the GMF for systems in fixed or mobile service using collinear antennas. This number is indicative of the extensive utilization of this type of antenna in the Government telecommunication systems.



(a) Electric Field



(b) Magnetic Field

Figure 4-32. Comparison of correction factor for E and H fields of a collinear antenna with full-wave dipole.



Electrically, a collinear antenna is an array of half-wave dipoles. Hence, the NEC program is very appropriate for analyzing this type of antenna. The NEC model was used to compare the E and H fields of a full-wave dipole with those for a collinear antenna. The results of the calculations are shown in Figure 4-32. Note that the correction factors for calculating the near electric and/or magnetic fields of a full-wave dipole are very nearly equal to those for a collinear antenna. Hence, the correction factors for a full-wave dipole may be used to assess the near field of a collinear antenna.

Summary of Results. The procedures developed in this section for calculating the E and/or H field intensities for the linear antennas discussed here are summarized in Table 4-5. The relationships for calculating E and H are

$$E = \frac{3.7}{\lambda} \sqrt{P_t G_t} (CF)_E \quad (4-16)$$

$$H = \frac{0.01}{\lambda} \sqrt{P_t G_t} (CF)_H \quad (4-17)$$

where:

$\lambda$  = Wavelength (meter)

$P_t$  = Transmitter power (Watts)

$G_t$  = Antenna gain

$(CF)_E$  = Correction factor for electric field

$(CF)_H$  = Correction factor for magnetic field

E = Electric field (Volts/meter)

H = Magnetic field (amperes/meter)

Equations 4-16 and 4-17 are general relationships and may be used in the near field assessment of any of the linear antennas described here. In these equations,  $G_t$ ,  $(CF)_H$ , and  $(CF)_E$  are the parameters that change from one antenna type to another.

TABLE 4-5 should be consulted in selecting the appropriate values for these parameters.

The curves in Figures 4-22, 4-23, 4-28, 4-30, and 4-32 include data for the parameters  $(CF)_E$  and  $(CF)_H$  in Equations 4-16 and 4-17. Note that the data in these curves may be used to evaluate the field intensities for distance less than  $1.5\lambda$ .

In the assessment of compliance of an antenna, the computation should begin with the far field equation

$$P_d = \frac{P_t G_t}{4\pi R^2} \quad (4-18)$$

If the calculation results show that the  $P_d$  is less than the level of acceptable criteria, then one should proceed with the near field assessment for distance smaller than  $1.5\lambda$ . For these calculations Equations 4-16 and 4-17 may be used in conjunction with the information in TABLE 4-5.

TABLE 4-5  
DESCRIPTION OF PARAMETERS USED  
IN EQUATIONS 4-16 AND 4-17

Antenna Name	$G_t$	$(CF)_E$	$(CF)_H$	Remarks
Dipole (freespace)	Dipole Gain	Correction factor of dipole electric field	Correction factor for dipole magnetic field	
Monopole	Monopole Gain	Correction factor for dipole in freespace	Correction factor for dipole in freespace	
Whip				Whip antenna can be a monopole or a collinear
Log Periodic	Gain of the log periodic	Same as the CF for a half-wave dipole	Same as the CF for a half-wave dipole	
Yagi	Gain of the Yagi	Same as the CF for a half-wave dipole	Same as the CF for a half-wave dipole	
Collinear	Gain of the collinear antenna	Same as the CF for a full-wave dipole	Same as the CF for a full-wave dipole	

APPENDIX A  
DEFINITION OF THE PARAMETERS IN TABLE 4-2

This appendix includes a brief description of the derivation and definition of the parameter used in the calculation of the correction factor for rectangular apertures as used in TABLE 4-2.

The Helmholtz potential function for rectangular aperture shown in Figure A-1 is expressed as:

$$P = \frac{1}{4\pi} \int_{-a}^a \int_{-b}^b J(r') \frac{e^{-jk|r-r'|}}{|r-r'|} dx' dy' \quad (A-1)$$

Where  $J(r')$  is the aperture distribution and the parameters  $a$ ,  $b$ ,  $r$ , and  $r'$  are defined in Figure A-1. The current distribution on the aperture was assumed to be uniform or cosinusoidal given by Equations 4-7 and 4-8. Substituting these distribution functions into Equation A-1, we obtain

$$P = \frac{1}{4\pi} \int_{-a}^a \int_{-b}^b \cos^n \left( \frac{\pi x'}{2a} \right) \cos^m \left( \frac{\pi y'}{2b} \right) \frac{e^{-jk|r-r'|}}{|r-r'|} dx' dy' \quad (A-2)$$

where  $n = 0, 1, 2, 3$ , and  $m = 0, 1, 2$ . The integral in Equation A-2 was evaluated for six different distribution functions listed in TABLE 4-2 by the appropriate selection of integers for the parameters  $n$  and  $m$ . The results of this evaluation are as follows:

- a. For uniform distribution ( $n=m=0$ )

$$P_{CO} = |P|^2 \quad (A-3)$$

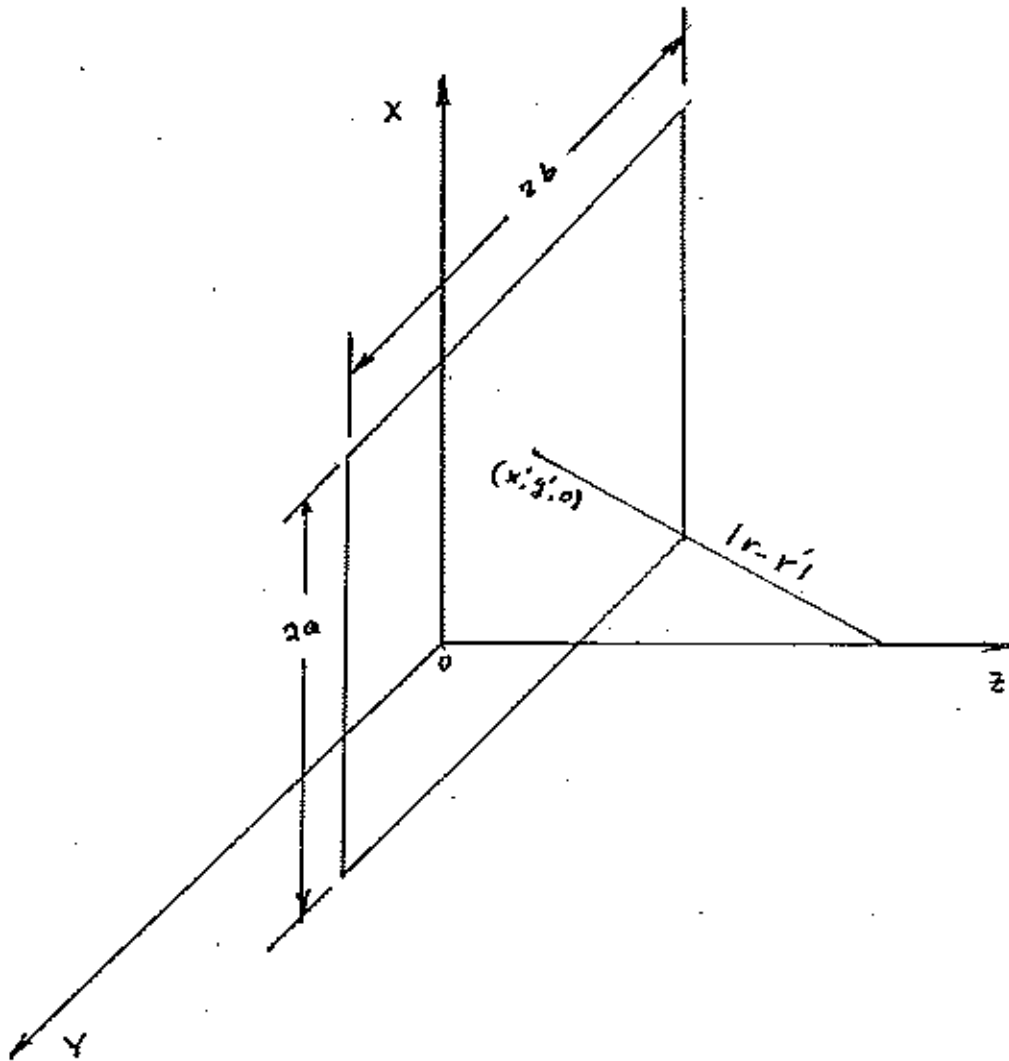


Figure A-1. Rectangular aperture geometry.

where:

$$P = Q[E_a E_b (1 + \frac{j}{2q\beta Q}) - \frac{j(D1 + D2)}{2qQ \sqrt{2\pi\beta}}] \quad (A-4)$$

and

$$D1 = a E_b \text{EXP} (-j\beta a^2) = a E_b e^{-j\beta a^2}$$

$$D2 = b E_a \text{EXP} (-j\beta b^2) = b E_a e^{-j\beta b^2}$$

$$j = \sqrt{-1}$$

$$E_a = C (\beta a^2) - jS(\beta a^2)$$

$$E_b = C (\beta b^2) - jS (\beta b^2)$$

$$q = z^2 + a^2 + b^2$$

$$\beta = \frac{\pi}{\lambda\sqrt{q}}$$

$\lambda$  = wavelength

$$Q = 1 + \frac{(a^2 + b^2)}{2q}$$

In Equation A-4, function C(v) and S(v) are cosine and sine integrals.

b. For cosine distribution (n=1 and m=0)

$$P_{c1} = |P_1|^2 \quad (A-5)$$

where:

$$P_1 = \frac{F_a E_b e^{\frac{j\pi^2}{16\beta a^2}}}{4} \left[ 2Q - \frac{\pi^2}{16\beta^2 q a^2} + \frac{j}{q\beta} - \frac{jbe^{-j\beta b^2}}{\sqrt{2\pi\beta q} E_b} \right] + \frac{\sqrt{\pi} E_b e^{-j\beta a^2}}{8\sqrt{2} q\beta^{3/2} a} \quad (A-6)$$

and

$$F_a = C(X_{1a}) - jS(X_{1a}) + C(X_{2a}) - jS(X_{2a})$$

$$X_{1a} = \beta a^2 \left( 1 - \frac{\pi}{4\beta a^2} \right)^2$$

$$X_{2a} = \beta a^2 \left( 1 + \frac{\pi}{4\beta a^2} \right)^2$$

c. For cosine squared distribution (n=2 and m=0)

$$P_{c2} = |P + P_{2a}|^2 \quad (A-7)$$

were:

$$P_{2a} = \frac{F_a E_b e^{\frac{j\pi^2}{4\beta a^2}}}{4} \left[ 2Q - \frac{\pi^2}{4q\beta^2 a^2} + \frac{j}{q\beta} - \frac{jbe^{-j\beta b^2}}{\sqrt{2\pi\beta} q E_b} \right] + \frac{j a E_b e^{-j\beta a^2}}{2q \sqrt{2\pi\beta}} \quad (A-8)$$

$$F_a' = C(X_{1a}') - jS(X_{1a}') + C(X_{2a}') - jS(X_{2a}')$$

$$X_{1a}' = \beta a^2 \left( 1 - \frac{\pi}{2\beta a^2} \right)^2$$

$$X_{2a}' = \beta a^2 \left( 1 + \frac{\pi}{2\beta a^2} \right)^2$$

d. For cosine cubed distribution ( $n=3$  and  $m=0$ )

$$P_{c3} = |P_3 + 3P_1|^2 \quad (A-9)$$

where:

$$P_3 = \frac{F_a E_b e^{\frac{j9\pi^2}{16\beta a^2}}}{4} \left[ 2Q - \frac{9\pi^2}{16q\beta^2 a^2} + \frac{j}{q\beta} - \frac{jbe^{-j\beta b^2}}{\sqrt{2\pi\beta} E_b q} \right] - \frac{3\sqrt{\pi} E_b e^{-j\beta a^2}}{8\sqrt{2} aq\beta^{3/2}} \quad (A-10)$$

and



$$F_a'' = C(X_{1a}'') - jS(X_{1a}'') + C(X_{2a}'') - jS(X_{2a}'')$$

$$X_{1a}'' = \beta a^2 \left(1 - \frac{3\pi}{4\beta a^2}\right)^2$$

$$X_{2a}'' = \beta a^2 \left(1 + \frac{3\pi}{4\beta a^2}\right)^2$$

e. For separable cosinusoidal distribution ( $n=m=1$ ):

$$P_{\text{oct}} = |P_{1c}|^2 \quad (\text{A-11})$$

where:

$$P_{1c} = \frac{F_a F_b e^{\frac{j\pi^2(\frac{1}{a^2} + \frac{1}{b^2})}{16}}}{4} \left\{ Q + \frac{1}{2q\beta} [J] - \frac{\pi^2(\frac{1}{a^2} + \frac{1}{b^2})}{16\beta} \right. \\ \left. + \frac{\sqrt{\pi}}{16\sqrt{2} q \beta^{3/2}} \frac{F_a e^{j(\frac{\pi^2}{16\beta a^2} - \beta b^2)}}{b} + \frac{F_b e^{j(\frac{\pi^2}{16\beta b^2} - \beta a^2)}}{a} \right\} \quad (\text{A-12})$$

$$F_b = C(X_{1b}) - jS(X_{1b}) + C(X_{2b}) - jS(X_{2b})$$

$$X_{1b} = \beta b^2 \left(1 - \frac{\pi}{4\beta b^2}\right)^2$$

$$X_{2b} = \beta b^2 \left(1 + \frac{\pi}{4\beta b^2}\right)^2$$

f. For separable cosine squared distribution (n=m=2)

$$P_{cc2} = |P + P_{2a} + P_{2b} + P_{2cc}|^2 \quad (A-13)$$

where:

$$P_{2b} = \frac{E_a F'_b e^{\frac{j\pi^2}{4\beta b^2}}}{4} 2Q - \frac{\pi^2}{4q\beta^2 b^2} + \frac{j}{q\beta} - \frac{j a e^{-j\beta a^2}}{\sqrt{2\pi\beta} q E_a} + \frac{j a E_b e^{-j\beta a^2}}{2q \sqrt{2\pi\beta}} \quad (A-14)$$

$$P_{2cc} = \frac{F'_a F'_b e^{\frac{j\pi^2}{4\beta} \left( \frac{1}{a^2} + \frac{1}{b^2} \right)}}{4} Q + \frac{1}{2q\beta} \left[ j - \frac{\pi^2}{4\beta} \left( \frac{1}{a^2} + \frac{1}{b^2} \right) + \frac{j}{4q \sqrt{2\pi\beta}} b F'_a e^{j \left( \frac{\pi^2}{4\beta a^2} - \beta b^2 \right)} + a F'_b e^{j \left( \frac{\pi^2}{4\beta b^2} - \beta a^2 \right)} \right] \quad (A-15)$$

$$F'_b = C(X'_{1b}) - jS(X'_{1b}) + C(X'_{2b}) - jS(X'_{2b})$$

$$X'_{1b} = \beta b^2 \left( 1 - \frac{\pi}{2\beta b^2} \right)^2$$

$$X'_{2b} = \beta b^2 \left( 1 + \frac{\pi}{2\beta b^2} \right)^2$$

## APPENDIX B

### COMPUTER PROGRAMS FOR CALCULATION OF NORMALIZED POWER DENSITY (CORRECTION FACTOR)

A description of the computer programs used in the calculation of normalized power density for aperture antennas is included in this appendix. Two types of aperture contours, i.e., circular and rectangular were considered in the analysis. RECAPE and CIRCAPE computer programs were developed for treating rectangular and circular apertures, respectively. These programs were written in Fortran and algorithms were based on the relationships developed here. A brief description of these programs and their input parameters are given in this appendix.

#### Circular Aperture Model (CIRCAPE)

The program CIRCAPE is used to compute and plot the normalized on-axis power density for different aperture sizes. The power density at the distance  $z$  along the aperture axis is normalized to the value of the power density at  $\frac{2D^2}{\lambda}$  where  $D$  is the diameter of circular aperture, and  $\lambda$  is the wavelength. The normalized power density referred to as the correction factor for an aperture is plotted as a function of normalized distance along the antenna axis. The distance along the axis is normalized to  $\frac{2D^2}{\lambda}$ .

The input parameters are:

RLD = Ratio of aperture radius to wavelength

EN = Exponent  $n$  in Equation (4-1)

The program has one subroutine for evaluation of an integral involving combination of polynomial and sinusoidal functions.

## Rectangular Aperture Model (RECAPE)

RECAPE is a computer program that may be used to compute and plot the normalized on-axis power density for rectangular apertures of different sizes. The aperture is in the x - y plane and the power density is calculated along the z axis. The calculated power density is normalized to the power density at  $\frac{8a^2}{\lambda}$  where 2a is the length of the aperture. The distance along the z axis is normalized to  $\frac{8a^2}{\lambda}$  which varies for 0.01 to 1.

The RECAPE program includes six different subprograms each for a different distribution function. This program is interactive and the user has to select the desired distribution of the list given below.

<u>Value of n</u>	<u>Distribution Function</u>
1	uniform
2	$\cos \left( \frac{\pi x'}{2a} \right)$
3	$\cos^2 \left( \frac{\pi x'}{2a} \right)$
4	$\cos^3 \left( \frac{\pi x'}{2a} \right)$
5	$\cos \left( \frac{\pi x'}{2a} \right) \cos \left( \frac{\pi y'}{2b} \right)$
6	$\cos^2 \left( \frac{\pi x'}{2a} \right) \cos^2 \left( \frac{\pi y'}{2b} \right)$

The input parameters for RECAPE are:

n = exponent for distribution function = 1, 2, ..., 6

AL = ratio of the length of aperture to wavelength  $\left( \frac{a}{\lambda} \right)$

BL = ratio of the width of aperture to wavelength  $\left( \frac{b}{\lambda} \right)$

The program has one subroutine for the evaluation of Fresnel integrals.

## BIBLIOGRAPHY

1. Adams, Arlon T., Thomas E. Baldwin, Jr., and Daniel E. Warren (1978), "Near Fields of Thin-Wire Antennas - Computation and Experiment," IEEE Transactions on Electromagnetic Compatibility, Vol. EMC-20, No. 1, February. The near fields of resonant dipole, broadside and endfire linear arrays are computed. The relevance of near-field computation to near-field radiation hazard is discussed.
2. Baker, A.E., and S. Mantel (1972), "Transmitter Nomenclatures and Calculated Power Densities for Selected Frequency Bands," ECAC, Annapolis, MD., June. Calculations were made of the power density at the near field peak, and the distance to the near field peak from the antenna.
3. Burnside, W.D., Nan Wang, and E.L. Pelton (1980), "Near Field Pattern Analysis of Airborne Antennas," IEEE Transactions on Antennas and Propagation, Vol. AP-28, May. Near-field patterns of an aperture or monopole antenna mounted on the fuselage of an aircraft are solved by the geometrical theory of diffraction.
4. Cleveland, Robert F. (1985), "Evaluation Compliance with FCC-Specified Guidelines for Human Exposure to Radiofrequency Radiation," Federal Communications Commission, Office of Science & Technology, Washington D.C., October. Calculations, measurements, tables and figures, and corrective actions to FM, TV, and AM broadcast facilities are provided. The FCC uses ANSI C95.1-1982 RF protection guides.
5. Farrar, Andrew, and A.T. Adams (1980), "An Improved Model for Calculating the Near Field Power Densities of Aperture Antennas," IEEE International Symposium on Electromagnetic Compatibility. Two computer algorithms for calculating the on-axis near field power densities of circular and rectangular aperture antennas for various illuminations are developed.
6. Fieni, Dino O. (1972), "Metropolitan Radiation Hazards," ECAC, Annapolis, MD., March. The transmitter environment contributing to radiation in Washington area is described.
7. Hansen, R.C. and L.L. Bailin (1959), "A New Method of Near Field Analysis," IRE Transactions on Antennas and Propagation 7, Special Supplement S458-S467, December. The accurate determination of the near field produced by a current distribution on a circular disc type aperture is examined.
8. Hansen, R.C. (1964), "Microwave Scanning Antennas, Volume I, Apertures," Academic Press Inc., New York, NY. The book contains much information on aperture distributions and near field theory.
9. Harrington, R.F. (1967), "Matrix Methods for Field Problems," Proceedings of the IEEE, Vol. 55, No. 2, pp. 136-149, February. The mathematical concept is the method of moments, by which the functional equations of electromagnetic field theory are reduced to matrix equations.

10. Harrington, R.F. (1968), "Field Computation by Moment Methods," MacMillian Company, New York, NY. The concept is the method of moments, which is the solution of electromagnetic field problems using computers.
11. Hu, Ming-Kuei (1961), "Fresnel Region Fields of Circular Aperture Antennas," Journal of Research of the National Bureau of Standards, Vol. 65D, 137-147, March. An approach using the Newton's iteration formula for square root is introduced to the Fresnel region field approximation.
12. Lee, S.H. (1980), "GTD Analysis of Reflector Antennas with General Rim Shapes - Near and Far Field Solutions," PH.D. Dissertations and Report 712242-4 (713742), Department of Electrical Engineering, the Ohio State University Electroscience Laboratory, Columbus, OH.
13. Mumford, W.W. (1961), "Some Technical Aspects of Microwave Radiation Hazards," Proceedings of the IRE, Vol. 49, No. 2, February. The safety limits of the Bell System are reviewed, and a method of calculating power densities is derived.
14. Office of Telecommunications Policy (1976), "Fourth Report on 'Program for Control of Electromagnetic Pollution of the Environment: The Assessment of Biological Hazards of Nonionizing Electromagnetic Radiation'," June. Effects of personnel exposure at relatively low power density levels, particularly over extended periods of time, and effects of use of the RF spectrum are described.
15. Polk, Charles (1956), "Optical Fresnel-Zone Gain of a Rectangular Aperture," IRE Transactions on Antennas and Propagation, Vol. AP-4, pp. 65-69, January. The on-axis gain of a uniformly illuminated rectangular aperture in the Fresnel Zone is compared with the gain of a circular aperture.
16. Rudduck, R.C., S.H. Lee, and W.D. Burnside (1979), "GTD Analysis of Reflector Antennas with General Rim Shapes," IEEE AP/S Symposium, Vol. 1, p. 71, Seattle, WA.
17. Schulz, Richard B. (1982), "Radiation Hazards Handbook," ECAC, Annapolis, MD., November. Radiation hazard limits concerning personnel, ordnance/explosives, fuel are summarized.
18. Silver, Samuel (1965), "Microwave Antenna Theory and Design," Dover Publications, Inc., New York, NY. Design of the primary feed and reflector to produce the aperture field is listed.
19. Stuart, William D. and Richard D. Albus, (1984), "Antenna Engineering Handbooks," ECAC, Annapolis, MD., December. Computer models capable of determining the near fields of linear antennas are described.
20. Tell, Richard A. and Edwin D. Mantiply (1980), "Population Exposure to VHF and UHF Broadcast Radiation in the United States," Proceedings of the IEEE Vol. 68, No. 1, January. A computer algorithm using broadcast signal field intensity measurement data for U.S. large cities estimates population exposure to broadcast radiation.

## REFERENCES

- Adams, A.T., Baldwin, T.E., and Warren, E., "Near Fields of Thin-Wire Antennas-Computation and Experiment", IEEE Transactions on Electromagnetic Comptability, Vol. EMC-20, No. 1, February 1978.
- Bickmore, R.W. and Hanson, R.C., "Antenna Power Densities in the Fresnel Region", IRE Proceedings, December 1959.
- Burke, G.J. and Poggio, A.J., "Numerical Electromagnetic Code (NEEC) - Method of Moments, A user Oriented Computer Code for Analysis of the Electromagnetic Response of Antennas and Other Metal Structures", Naval Ocean System Center, San Diego, California 92152, NOSC TD 116, Vol. 1, (September 1980).
- Burnside, W.D., Rudduck, R.C. and Marhefka, R.J., "Summary of GTD Computer Codes Developed at the Ohio State University", IEEE Trans. EMC, Vol. 22, pp. 238-243, November 1980.
- Cleveland, R.F., "Evaluating Compliance with FCC-Specified Guidelines For Human Exposure to Radio Frequency Radiation", OST Bulletin No. 65 Federal Communication Commission, Washington, D.C. 20554 (October 1985).
- Farrar, A., and Adams, A., "An Improved Model for Calculating the Near Field Power Densities of Aperture Antennas, Symposium Digest", IEEE 1980 Electromagnetic Compatibility (1980).
- Farrar, A., Dobson, H., and Wentland, F., "Evaluation Techniques-Fixed Service Systems to Power-Line-Carrier Circuits", NTIA Report 85-181, U.S. Department of Commerce, (Sept. 1985).
- Harrington, R.F., "Field Computation by Moment Methods. New York: Macmillan Co., 1968.

REFERENCES (continued)

Harrington, R.F., "Matrix Methods of Field Problems", Proc. IEEE, Vol. 55, No. 2, February 1967, pp. 136-149.

Harrington, Roger F., "Time-Harmonic Electromagnetic Fields", McGraw Hill Book Co., N.Y. 1961.

ITT, Harad book (1975)

Jordan, E.C. and Balmain, K.G., "Electromagnetic Waves and Radiating Systems", Prentice Hall Inc., N.J. (1968).

Kraus, J.D., "Antenna" McGraw Hill Book Co. Inc., N.Y. 1950.

Lee, S.H., "GTD Analysis of Reflector Antennas with General Rim Shapes-Near and Far Field Solutions", Ph.D. dissertation and Report 712202-4 (713742), The Ohio State University ElectroScience Laboratory, Department of Electrical Engineering; prepared under Contract No. N00123-79-C-1469 for Naval Regional Procurement Office, Sept. 1980.

Lee, S.H. and Rudduck, R.C., "Numerical Electromagnetic Code (NEC)-Reflector Antenna Code. Part II: Code Manual", Report 784508-16, The Ohio State University ElectroScience Laboratory, Department of Electrical Engineering; prepared under Contract No. N000123-76-C-1371 for Naval Regional Procurement Office, Sept. 1979.

Navsea OP 35 65/Naviar 16-1-529/Navelex 0967-LP-624-6010, Volume 1 fifth revision.

[NTIA, 1986], Manual of Regulations and Procedures for Federal Radio Frequency Management, U.S. Department of Commerce, National Telecommunications and Information Administration, Washington, D.C. May 1986 Edition.



REFERENCES (continued)

Silver, S. "Microwave Antenna Theory and Design", Dover Publication, Inc., New York, 1965.

Skolnik, M.I., "Radar Handbook", McGraw Hill Book Co., N.Y. 1970.

TO 31Z-10-4 Army FM 11-490-30, (AF) TO 31Z-10-4 (Army) FM 11-490-30.

## BIBLIOGRAPHIC DATA SHEET

1. PUBLICATION NO. NTIA TM-87-129		2. Gov't Accession No.	3. Recipient's Accession No.
4. TITLE AND SUBTITLE PROCEDURES FOR CALCULATING FIELD INTENSITIES OF ANTENNAS		5. Publication Date September, 1987	
		6. Performing Organization Code	
7. AUTHOR(S) Andrew Farrar, Eugene Chang		9. Project/Task/Work Unit No.	
8. PERFORMING ORGANIZATION NAME AND ADDRESS National Telecommunications & Information Administration 179 Admiral Cochrane Drive Annapolis, Maryland 21401		9017171	
		10. Contract/Grant No.	
11. Sponsoring Organization Name and Address U.S. Department of Commerce/NTIA 179 Admiral Cochrane Drive Annapolis, Maryland 21401		12. Type of Report and Period Covered Technical	
		13.	
14. SUPPLEMENTARY NOTES			
15. ABSTRACT (A 200-word or less factual summary of most significant information. If document includes a significant bibliography or literature survey, mention it here.) This report discusses simplified procedures for calculating near and far field intensities of several types of aperture and wire antennas. The antenna technical characteristics listed in the Government Master File (GMF) were reviewed. For this analysis, two categories (i.e., linear and aperture) were found to be sufficiently representative of the majority of antenna types listed in the GMF. Existing analytical antenna models developed for a near field analysis of the antennas were identified. Some of these models were used to develop a simplified model for estimating near field radiation from Government radiocommunications systems. These models are conservative and are expected to yield higher field intensity or power density values than would be expected in actual practice. Measurements may be required to determine more exact values for these parameters.			
16. Key Words (Alphabetical order, separated by semicolons) ANTENNAS COMPUTER MODELS LINEAR AND APERTURE ANTENNAS MODELS FOR NEAR FIELD ANALYSIS NEAR FIELD ANALYSIS FOR ANTENNAS RADIO FREQUENCY RADIATION HAZARD ASSESSMENT			
17. AVAILABILITY STATEMENT <input type="checkbox"/> UNLIMITED <input type="checkbox"/> FOR OFFICIAL DISTRIBUTION		18. Security Class. (This report) Unclassified	20. Number of pages 97
		19. Security Class. (This page) Unclassified	21. Price: